

Online Research @ Cardiff

This is an Open Access document downloaded from ORCA, Cardiff University's institutional repository: <https://orca.cardiff.ac.uk/id/eprint/127556/>

This is the author's version of a work that was submitted to / accepted for publication.

Citation for final published version:

Stein, William E., Berry, Christopher M. ORCID: <https://orcid.org/0000-0001-9521-5618>, Morris, Jennifer L. ORCID: <https://orcid.org/0000-0002-7453-3841>, VanAller Hernick, Linda, Mannolini, Frank, Ver Straeten, Charles, Landing, Ed, Marshall, John E. A., Wellman, Charles H., Beerling, David J. and Leake, Jonathan R. 2020. Mid-Devonian archaeopteris roots signal revolutionary change in earliest fossil forests. *Current Biology* 30 (3) , 421-431.e2. 10.1016/j.cub.2019.11.067 file

Publishers page: <http://dx.doi.org/10.1016/j.cub.2019.11.067>
<<http://dx.doi.org/10.1016/j.cub.2019.11.067>>

Please note:

Changes made as a result of publishing processes such as copy-editing, formatting and page numbers may not be reflected in this version. For the definitive version of this publication, please refer to the published source. You are advised to consult the publisher's version if you wish to cite this paper.

This version is being made available in accordance with publisher policies.

See

<http://orca.cf.ac.uk/policies.html> for usage policies. Copyright and moral rights for publications made available in ORCA are retained by the copyright holders.



**MID DEVONIAN *Archaeopteris* ROOTS
SIGNAL REVOLUTIONARY CHANGE
IN EARLIEST FOSSIL FORESTS**

William E. Stein^{1,6,7,*}, Christopher M. Berry^{2,6}, Jennifer L. Morris^{2,6}, Linda VanAller Hernick³,
Frank Mannolini³, Charles Ver Straeten³, Ed Landing³, John E. A. Marshall⁴, Charles H.
Wellman⁵, David J. Beerling⁵, and Jonathan R. Leake⁵

¹Department of Biological Sciences, Binghamton University, Binghamton NY 13902

²School of Earth and Ocean Sciences, Cardiff University, Cardiff, CF10 3AT, UK

³New York State Museum, Albany, NY 12230

⁴School of Ocean and Earth Science, University of Southampton, Southampton SO14 3ZH, UK

⁵Department of Animal and Plant Sciences, University of Sheffield, Sheffield S10 2TN, UK

⁶These authors contributed equally

⁷Lead Contact

*Correspondence: stein@binghamton.edu (W.E.S.), BerryCM@cardiff.ac.uk (C.M.B.),
drjenlmorris@gmail.com (J.L.M.).

SUMMARY

The origin of trees and forests in the Mid Devonian (393-383 Ma) was a turning point in Earth history marking permanent changes to terrestrial ecology, geochemical cycles, atmospheric CO₂ levels and climate. However, how all these factors interrelate remains largely unknown. From a fossil soil (palaeosol) in the Catskill region near Cairo NY, USA we report evidence of the oldest forest (mid Givetian) yet identified worldwide. Similar to the famous site at Gilboa NY, we find treefern-like *Eospermatopteris* (Cladoxylopsida). However, the environment at Cairo appears to have been periodically drier. Along with a single enigmatic root system potentially belonging to a very early rhizomorphic lycopsid, we see spectacularly extensive root systems here assigned to the lignophyte group containing the genus *Archaeopteris*. This group appears pivotal to the subsequent evolutionary history of forests due to possession of multiple advanced features and likely relationship to subsequently dominant seed plants. Here we show that *Archaeopteris* had a highly advanced root system essentially comparable to modern seed plants. This suggests a unique ecological role for the group involving greatly expanded energy and resource utilization, with consequent influence on global processes much greater than expected from tree size or rooting depth alone.

INTRODUCTION

Trees play an exceedingly complex structural and biotic role within modern terrestrial forest ecosystems [1]. Although Carboniferous (359-299 Ma) fossil forests included tree-sized lycopsids, sphenopsids and ferns [2,3], seed plants have overwhelmingly populated terrestrial forests since the late Paleozoic. However, during the critical interval of initial establishment of Earth's earliest forests, the Mid Devonian, all trees have uncertain evolutionary relationships [4] and are incompletely understood. As a result, direct fossil evidence is critically needed to understand factors relating to initial terrestrial ecosystem assembly, including data on habitat specificity, spatial distributions, ecological tolerances, rooting behavior, and plant interactions [5,6]. Paleosols mapped in plan view potentially provide some of this key information. From

Riverside Quarry, Gilboa, New York, trees identified as *Eospermatopteris* [7], with *Wattieza* foliage (belonging to extinct order Pseudosporochneales, class Cladoxylopsida) [8], were previously shown to occur as forest dominants associated with other tree-sized forms including procumbent to lianoid aneurophytaleans (cf. *Tetraxylopteris*, class Progymnospermopsida) and at least one arborescent probably cormose lycopsid [9]. All root systems at Gilboa were simple sparsely branched linear structures generally typical of plants of this and earlier age. However, archaeopteridaleans were conspicuously missing. Commonly placed within the single genus *Archaeopteris* (= *Callixylon*), the group shows significant variation, and very likely represents a taxonomically diverse as well as ecologically significant forest element [10]. Moreover, archaeopteridaleans possess an impressive set of seed plant features assembled together for the first time in the fossil record, including large upright habit, eustelic primary vascular system, bifacial vascular cambium producing conifer-like secondary tissues, laminate leaves, heterospory, delayed development involving bud-like behavior, and endogenous root production [11-13]. Macrofossil and microfossil evidence suggests appearance of *Archaeopteris* worldwide by the early Givetian (388-383 Ma), with apparent rise to dominance in the Catskill region by the Famennian (372-359 Ma) [14,15]. Reconstructed with conifer-like form [16,17] and given its widespread occurrence, *Archaeopteris* has commonly been assumed to occupy drier habitats compared to potentially more ecologically restricted *Eospermatopteris* [10], but direct evidence for the ecological amplitude for either tree, and consequent influence on global processes, remains unknown.

RESULTS

From a paleosol in an abandoned quarry in the Plattekill Formation of the Hamilton Group near Cairo, NY (42°19'09.23"N, 74°02'40.16"W), we have uncovered evidence for a strikingly

different paleoenvironment than Riverside Quarry Gilboa, that now includes *Archaeopteris* (Figure 1). Strata at the site are interpreted to be correlative with the marine Ludlowville Formation to the west, which is early mid Givetian (ca. 385 Ma) in age [18] and ca. 2-3 Ma older than Riverside Quarry in the Cooperstown (Moscow) Formation, dependent on time scale used [19,20]. Plant fossils found over many years of collecting in the quarry include the common major groups of Middle Devonian plants (aneurophytaleans, archaeopteridaleans, cladoxylopsids, lycopsids) [21,22], as well as restricted horizons containing liverworts and vertebrate fragments [23,24]. A portion of the quarry floor provides an extensive plan exposure of a siltstone horizon interpreted as the upper part of a paleosol containing spectacular *in situ* root systems (Figure 1C).

Paleosol Description and Interpretation

To date approximately 3000 m² surface of the paleosol has been uncovered. Most regions show complex texture with heavy fracturing into small 1-3 cm blocks as a result of recent weathering and past quarrying. This pattern is superimposed on larger slickensided curvilinear fractures that form semi-spheroidal features 10-30 cm in diameter. In addition, the surface undulates, with many small to larger-scale holes and semi-circular depressions, some of which may represent smaller paleofloral elements that cannot be identified as such, or variations in surface topography. There is also considerable lateral variation in color across the mapped paleosol surface. In the north part of the exposure (Figure 1C, region I), the root systems penetrate a siltstone predominantly dusky to weak red in color (Munsell colors 10R 5/4 – 10R 3/3), with patchy bluish-gray mottling (10B 6/1). This mottling is related in part to the occurrence of nearby root systems, and many root traces exhibit bluish-gray haloes (Figures 3C-F). To the south-southwest (Figure 1C, region II), the mottling intensifies until the siltstone becomes

entirely gray (10B 6/1 - N 6/). In these areas, the siltstone contains abundant organic plant material showing by far the best-preserved roots. Occurring here is a spectacular tree root system showing conspicuous limonite (iron oxide) surface incrustations and numerous exposed smaller roots (Figures 4C, 5). Further in the same direction (Figure 1C, region III), abundant limonite appears within the paleosol matrix (Figure 4C). In both occurrences, limonite has intensified in color (5YR 6/4) after uncovering and almost certainly represents modern oxidation of early diagenetic pyrite. In another region (Figure 1C, region IV), a thin siltstone layer with a distinctive greenish color (10G 6/1) overlies the mottled paleosol surface. It is at least 10 cm thick to the east, but feathers out to the north and southwest. In this area, root systems appear on the underlying paleosol, but are invested by the greenish siltstone forming partial molds (Figures 3A-B, 4A-B). Beyond the region of continuous deposition, the same greenish siltstone occurs as isolated patches apparently trapped by root systems of the largest plants near their center (Figure 5A). The greenish siltstone has scattered vertebrate fragments (placoderms, agnathans, chondrichthyans) on the surface (Figure 4D) and several well-articulated fish have been recovered near the largest trees, seemingly impounded by them. This siltstone is interpreted as overwash from a flood event that penetrated the forest from the east, likely killing many trees and preserving root systems as trace fossils.

From data derived from cores drilled at the site, the surface-mapped paleosol (Figures 2A-B, PII) ranges between 1.20 and 1.66 m in thickness, with a gradational lower boundary into either finely-laminated grayish-red (10R 5/3) 'heterolithics' (interbedded mudstone, siltstone and fine-grained sandstone Figure 2B, R), or an underlying paleosol profile (Figures 2A-B, PIII-PIV). The paleosol is capped with the same overwash siltstone seen on the surface, with sharp lower boundary but without a significant change in grain size or evidence of a significant erosional

115 surface. Within the paleosol ([Figure 2B, PII](#)), 3 horizons (A-C), with variants: A(g), (AE), B,
116 Btss, Bt, C, are recognized across the mapped area, all with abundant evidence of rooting.
117 Horizon A is a siltstone between 12 and 25 cm thick, has a massive structure, and granular to
118 sub-angular blocky texture of peds. It is either red, partially gleyed to a bluish-gray color from
119 the surface downwards, or is entirely gleyed (Ag), where small patches of pyrite have been
120 found. In a few cores, an additional subhorizon, AE, occurs at the base of Horizon A where the
121 matrix is significantly lighter in color (10R 6/4). Horizon B is between 56 and 118 cm thick, and
122 is characterized by increased clay content and larger, more angular, blocky to columnar peds
123 separated by significant cracks. Conspicuous is subhorizon Btss, a clay-rich layer comprising
124 blocky, wedge-shaped peds with slickensided argillaceous cutans. Horizon C, between 11 and 40
125 cm thick, is characterized by a clayey siltstone with a massive texture, root traces and incipient
126 bedding.

127 From observations of both surface and cores, the mapped surface ([Figures 1C; 2, PII](#)) is
128 interpreted as a single vertisol, based on horizon properties, specifically sub-horizon Btss which
129 is indicative of this soil order [[25,26](#)]. Movement along pseudo-anticlinal slip planes produced
130 the slickensided wedge-shaped peds and the semi-spheroidal features observed at the surface.
131 These slip planes developed with the shrinking and swelling of clays, as a result of wetting and
132 drying seasonal cycles [[27](#)]. Variable gleying at the top of the paleosol is interpreted as
133 reflecting variable short term surface waterlogging across the forest, likely associated with
134 flooding with emplacement of fish, localized topographic differences, or proximity to a water
135 source.

Identified Root Systems

Eospermatopteris

Three root systems, two unique to this site, have been identified to date. The first type (Figures 1C, arrows a-b; 3) is fully equivalent in form and detail to root systems at Gilboa [7-9], with that site also including stem casts previously identified as *Eospermatopteris* [7-8]. At Cairo, bowl-shaped depressions 20-50 cm in diameter were made by expanded bases of an upright trunk. Roots, inserted on the bottom and sides of the base, radiate sub-horizontally and form a densely imbricate pattern that disappears below the paleosol surface 1-2 m from the center. Roots are 0.7–1 cm in diameter, smooth to longitudinally plicate, and rarely if at all branched. One exceptional example (Figures 1C, arrow a; 3A-B) shows a well-preserved external mold of the trunk base directly seated on the PII paleosol with root surface features partly cast by the overlying greenish overwash siltstone. Roots extend from the base into the overwash and also downward into the underlying paleosol suggesting that the tree remained erect during the flood and may have remained viable for sometime thereafter. Other individuals in the overwash region show much less evidence of siltstone envelopment possibly related to differences in original pre-flood surface topography, flood sediment thickness or post-flood establishment of some trees. Outside the overwash region (Figures 1C, arrow b; 3C-F), *Eospermatopteris* root systems show somewhat less depressed central bowls surmounting raised mounds on the paleosol surface (Figures 3C-D). In several cases, a partial to nearly complete boundary in the root mass is marked by near vertical slickensided surfaces (Fig. 3A, arrows; 3D, arrows), although roots from the trees penetrate into the paleosol well beyond this distance and up to 30 cm depth. The slickensided boundary is interpreted as recording differences in paleosol shrink-swell movement between sediment bound within the root mat versus less cohesively bound peripheral regions.

(See the supplemental data for measurements of *Eospermatopteris* root systems found at the site.)

Archaeopteris

By far the most conspicuous root systems at Cairo have radial dimensions as much as 11 m across the paleosol surface and show great complexity (Figure 1C, arrows d-e; 5-6). As many as 10-15 primary roots resulting from numerous divisions diverge from what were probably bases of single central trunks. Some root systems appear essentially symmetrical (Figure 4A) whereas others show marked directionality (Figure 4C). The primary roots range between 6-16 cm in diameter, although fidelity of preservation and casting by overlying sediment contribute to imprecision in measurement. Root pattern, primary root diameters, and radial extent of primary roots suggest trees of different sizes (See Supplemental Figure S6, Supplemental Table S1). Root systems in the overwash region of the site (Figures 1C, arrow d; 4A-B) are especially conspicuous due to casting by the overlying greenish siltstone. However, these roots are evidently seated upon the PII paleosol below, and show only the largest surficial roots with occasional dichotomous branching. Associated root traces in the cores penetrate the paleosol to a depth of 1.2-1.6 m, with positive association between depth and estimated tree size (Figures 2C-D).

The most fully articulated detail of this type of tree is provided by a directional root system in gray paleosol diverging mostly to the south-southwest (Figures 1C, arrow e; 4C). Center of the root system is an irregular region with large primary roots as much as 15 cm in diameter. A small region of red-gray mottled paleosol occurs in high relief likely forced upward from the original rooting surface by the tree's weight (Figure 5A, arrows). In addition, a small amount of overwash siltstone caps the highest surfaces suggesting accumulation against the standing tree

182 some 7 m beyond the limit of contiguous overwash. Away from the center, the primary roots are
 183 observed to branch both equally and unequally, producing a highly ramified system that is only
 184 partly exposed on the surface ([Figures 5B-C](#)). Root cloning is suggested by radiating patterns of
 185 larger and smaller root systems both here and elsewhere at the site ([Figure 4C, arrow](#)), but
 186 definitive evidence for this is lacking. Working outward 2, 4, 6, and 8 m from the center, roots
 187 show progressive diminishment in root diameters (6-7 cm, 5-6 cm, 4-5 cm, 2.5-3.5 cm
 188 respectively) with individual root segments sometimes also showing modest taper between
 189 apparent branch points. Some surfaces show limonite incrustations ([Figures 5C](#)), and some have
 190 blocky transverse-longitudinal in-filled cracks ([Figure 5G](#)) reminiscent of wood checking. At ca.
 191 4-6 m from the center, anisodichotomous branching predominates in the root system, resulting in
 192 numerous lateral roots typically 1-1.5 cm in diameter. Some of these ([Figures 5D, 5F](#)) exhibit
 193 many small 1-2 mm diameter attached rootlets that diverge at angles ranging from acute to near
 194 90°. At more than 8 m from the center, the terminus of one major root is observed. Here, a
 195 raised semi-circular fan is evident on the paleosol surface bounded by a subvertical slickenside
 196 distal margin ([Figures 5E, arrows](#)), again interpreted as the boundary between root-bound
 197 sediment and adjacent paleosol. Extending at least 10 m from the center of this individual, and
 198 observed associated with another root system of this type nearby ([Figure 1C, arrow f](#)), are ca. 1
 199 mm diameter rootlets apparently comprising a dense three-dimensional mat. Rootlets typically
 200 enclose 1-3 cm diameter ped-like elements of the paleosol and are interpreted as the finest
 201 portions of a still largely intact, feeder root system. (See [Supplemental data](#) for measurements,
 202 and [Table S1](#) estimates of tree sizes).

203 Although our understanding of the relationship between Devonian plant body fossils and the
 204 trace fossils left by their root systems in paleosols is currently rudimentary, all features match

what we know or reasonably presume to be present in *Archaeopteris* and no other taxon so far identified in the Middle Devonian flora of the Catskills or worldwide. Notable is the presence of structural roots showing taper suggesting secondary development. Significant inequality in branching is consistent with production of laterals of different ages with differing amounts of secondary xylem. The presence of numerous small rootlets associated and attached to distal portions of an evident system of structural roots suggests continuous production of a feeder system consistent with previously described endogenous root development in *Archaeopteris* from anatomically preserved material [11,13,28].

Stigmarian Isoetalean Lycopsid?

A third and currently enigmatic type of tree is represented by a single well-preserved root system occurring largely within the dark grey paleosol region (Figures 1C, arrow c; 6). This system has a nearly circular raised root mound 1.9 m in diameter that is marked at the periphery by a slickensided distal margin similar to that described above for *Eospermatopteris* (Figure 6C, arrows). However, the center also exhibits a low 3-4 ridged depression 80 cm in diameter and clearly attached primary roots with diameters of 12, 15 and 25 cm at their insertion, the largest representing a proximal dichotomy (Figure 6B, arrows). A densely imbricate system of rootlets ca. 1 cm in diameter is well preserved as casts, and several show direct attachment to the primary roots toward the periphery of the root mound (Figure 6D). Other rootlets appear to radiate from the central depression suggesting direct attachment to the stem base. Beyond the root mound, the large primary roots, 5-6 cm in diameter, are observed in organic connection stretching along the paleosol surface as much as 13 m (Figure 6A). The primary roots show sparse equal dichotomies resulting in a lax distal system of secondary roots ca. 3-5 cm in diameter, with some extending into the limonitic region III to the south-southwest. Occasional carbon flecks

occurring in regular patterns along a secondary root length suggest attachment sites of rootlets at most levels (Figure 6E, arrows). In one instance, a secondary root was followed to the root tip. At this level it is invested by attached, but fragmentary, 0.7 cm diameter rootlets with fine scale longitudinal surface striations diverging at acute angles (Figure 6F, arrows).

Although observed from only a single occurrence at Cairo, evidence for a third type of tree at the site is nevertheless convincing. Among known Mid Devonian plants, nothing yet shows comparable features. However, as our terminology suggests, comparison with stigmarian isoetalean lycopsids of the Carboniferous seems the closest match.

DISCUSSION

Environmental Setting of the Riverside Quarry Gilboa and Cairo Sites

The Gilboa and Cairo sites, close in age but showing contrasting paleosol evidence, provide important glimpses into the general ecology of some of the Earth's early forests. Both sites occur within a familiar range of sediment types preserved in the Catskill Delta complex [29], and it seems likely that both are components of the same distal floodplain system in a subtropical to temperate wetland environment during an interval of relatively high sea level in the Appalachian Basin [19,30]. Multiple stacked ca. 1m thick sandstone horizons at the Riverside Quarry Gilboa, sometimes bearing rooted *Eospermatopteris*, likely indicate a terrestrial wetland environment for the trees, punctuated by disturbance [9]. At somewhat larger scale, the Schoharie valley, containing both Riverside Quarry and nearby Manorkill Falls [31], shows incursions of fully marine waters as indicated by intercalated units with marine invertebrates [32]. However, fish fragments are rare, and within the Riverside Quarry itself the massive sandstones lack any evidence of marine influence. Micro- and macro-morphological studies of the Gilboa and

Manorkill Falls forest soils [9,28,31] suggest poor drainage and high water tables as indicated by extensive gleying, drab colors, large amounts of organic carbon, and abundant pyrite.

At Cairo, low angle cross-bedded sandstones exposed in the quarry walls occur immediately above a mudstone containing the acritarch *Veryhachium*. The latter indicates some marine influence from, perhaps, tidal and wave-affected channels [33]. However, marine macrofossils are absent anywhere in the quarry. Based on our observations, it seems likely that a single event of flooding brought sediment and fish into an otherwise tree-dominated terrestrial ecosystem. The presence of chondrichthyans in the greenish overwash suggests marginal marine or brackish origin, and this is further supported by the presence of leiospheres [34] known to be abundant in near shore and lagoonal environments [33]. Several horizons, including an extensive black shale unit bearing conchostrachans and liverworts in another part of the quarry (Fig. 1B, arrow), suggest the presence of nearby lacustrine environments. In contrast to Gilboa, the red vertisols underlying part of the Cairo forest (Fig. 1C, regions I & IV) indicate well-drained soils with periodic wet/dry seasonality, but less disturbance overall. In addition, a wetter local environment is suggested by sediments with more extensive gleying (Fig 1C, regions II-III), perhaps supported by preferred directions of root systems in the direction of greatest pyrite deposition (Fig. 1C, c and e, region III).

Role of Major Groups in the Catskill Early Terrestrial Ecosystem

Cladoxylopsids - The presence of *Eospermatopteris* at Riverside Quarry, Manorkill Falls, and at Cairo suggest that these plants had the capacity to live in several different ecological settings rather than being restricted to wetter environments as has been previously interpreted. Their upright habit includes extensive augmentation of tissues by means of extended lateral meristem development [35], but limited sclerified tissues. Thus, it seems more likely that these plants

were weedy in habit, relatively fast growing, and able to disperse to a variety of locations in the ancient forest as chance, local disturbance, or openings in the forest canopy might have allowed.

Aneurophytaleans - By contrast, aneurophytaleans observed at Gilboa, and generally common in Catskill sediments as aerial shoots, produced both secondary xylem and phloem [36] similar to that seen in seed plants. Developmental evidence, however, suggests that secondary tissue production was probably limited [37], and it seems likely that most specimens found so far represent determinate portions of the plants that completed development with sterile or reproductive ultimate units, or a mixture of the two [38]. However it remains uncertain how these plants actually grew. The Gilboa paleosol provides evidence that aneurophytaleans were scrambling to ascendant tree sized forms with a rhizomatous to lianoid main axis not yet identified from anatomical material [9]. Aneurophytalean aerial shoots are represented as both compressions and pyrite permineralizations at Cairo [21,22], but main axes with surface features as observed at Gilboa have not been recognized from the paleosol horizon itself. This may be due to insufficient preservation of diagnostic details (see especially blocks L26-P29 in Fig. 1C from a probably wetter environment perhaps more similar to that Gilboa).

Lycopsids - Despite commonly held perspective holding to a *Lycopodium*-like interpretation for most Devonian lycopsids, rhizomes and root structures remain largely unknown. Many if not most of the most conspicuous occurrences in Catskills sediments appear to be detrital in origin [39,40]. Similar to aneurophytaleans, this leaves open how Middle Devonian lycopsids should be reconstructed, how big most of them were, and what roles they may have played in the structure of early forests. A tree-sized lycopsid was recovered from the paleosol at Riverside Quarry Gilboa and, although incomplete, probably had a cormose base [9]. This type of base is well preserved in *Lepidosigillaria* from the mid Frasnian of New York [41], and in individuals

from a newly described lycopsid forest from the early Frasnian of Svalbard [42]. By contrast, stigmarian lycopsid root systems involving elongate roots with appendicular rootlets make their body-fossil appearance in the Late Devonian (Famennian) [43]. Although wetland specializations are famous for both groups in the Carboniferous [2], there seems to be little if any evidence for similar environments in the Middle Devonian. The potential lycopsid root system observed at Cairo seems consistent with what one might expect of a stigmarian isoetalean lycopsid and would be the oldest occurrence yet described worldwide. Although suggestive, it must be admitted that evidence remains inconclusive pending confirmation with body fossils. If true, however, lycopsids may have been much larger and far more important as trees in forests much earlier than generally recognized, but in environments at least spanning those observed at Gilboa and Cairo.

Pivotal Role of *Archaeopteris* in Emerging Terrestrial Ecosystems

Eospermatopteris bases as at Gilboa and Cairo indicate that their roots were typically shallow (Figure 2E), and although the individual roots may have been meters in length, there is little indication that these were multi-year perennial structures. Thus with continued growth of the tree, active roots would have required regular replacement at a rate commensurate with augmentation of aerial tissues. However, new roots and the root system as a whole would have been largely restricted to reworking soils in the vicinity of the plant's main axis. Although rhizomatous and clonal plants would have permitted some lateral movement across the landscape, nevertheless similar restrictions appear characteristic of Devonian plants in general. In striking contrast, the root systems here assigned to *Archaeopteris* mark a dramatic departure from this pattern and, moreover, appear essentially indistinguishable from what might be observed in modern seed plants [44,45]. In modern woody trees there is typically a two-fold

investment strategy that includes progressive recruitment, extension, and maintenance of perennial structural roots along with seasonal renewal of smaller ephemeral feeder rootlets in a flexible and potentially ever-expanding array. Evidence at Cairo suggests that the root system of *Archaeopteris* probably functioned in much the same way, signaling a dramatic increase in rooting complexity and extent compared with contemporaneous land plants. Moreover, it seems likely that supplying an ever increasing distal root biomass over the lifetime of the individual would only be possible given augmentation of vascular system via indeterminate secondary tissues. The innovation of leaves, also in *Archaeopteris*, suggests greatly increased photosynthetic receptive surface area per unit biomass compared to contemporaneous plants with non-laminate appendages. This, combined with other derived features occurring together for the first time in *Archaeopteris*, points to tight developmental integration producing a clade-specific quantum leap in physiological capacity of these trees involving rates of energy capture and local resource utilization. Thus, it seems likely to us that this change was fundamental to the subsequent success of *Archaeopteris* and the entire lignophyte clade including seed plants in most terrestrial environments.

Previous work has emphasized the importance of roots in “bioengineering” important geochemical cycles associated with “afforestation” of the Earth [46-50]. We see at Cairo that maximum root depth for *Archaeopteris*, but not *Eospermatopteris*, is indeed related to tree size and root lateral extent (Figure 1C-E), as previously suggested [11]. However, since these trees co-occur within the same paleosol, it is clear that the effect of rooting patterns on paleosol development and potential weathering should now be seen to be taxon specific. Beyond that, the enhanced physiological package observed in *Archaeopteris* suggests multiplicative effects on both local environments and global processes well beyond that scaled to forest tree size or

rooting depth alone. As a result, it now becomes especially important to consider more fully how these enhanced trees flourished on the ancient Devonian landscape, and changed in both geographic range and ecological amplitude over time. In our opinion, previous ecological interpretations of *Archaeopteris*, and indeed all Mid Devonian plant groups, needs to be reassessed. Given extensive root systems supported by woody tissues, it seems likely that a stable soil environment, perhaps periodically wet and dry as seen at Cairo, would be necessary for *Archaeopteris* to grow to tree size and significant forest dominance. Just as today, it seems likely that these trees plus other plants in early forests, local topography, geographic setting, weathering, and geochemical cycling had multifaceted interrelationships. Thus, understanding what effect the energetic revolution represented by *Archaeopteris* may have had at global scale, including climatic change or extinction, needs to be informed by a more realistic appraisal of these factors in both local ecosystems and at regional scales. Understandably, unraveling all these factors is a tall order! However, what is clear from the occurrence of *Archaeopteris* at Cairo is that this is a Middle Devonian problem, far earlier than previously suspected. In addition, linking different environments based on paleosols with specific plant assemblies as done with Riverside Gilboa and Cairo may provide an enhanced tool for regional landscape and forest reconstructions. The latter is seemingly a prerequisite for assessing temporal changes in larger scale processes. Clearly two examples of this type from sites only 40 km apart are not enough. The essential point is that taxon-specific physiology and ecosystem composition, not just tree size, must now be considered vital keys to understanding the dramatic effect the origin of forests had on planet Earth.

ACKNOWLEDGEMENTS

Drilling costs were met by Natural Environment Research Council (NERC of Great Britain) Grants NE/J007471/1, NE/J007897/1 and NE/J00815X/1. Authors thank the Town of Cairo, and

Town of Cairo Highway Department for granting access and enthusiastic help with their site, also thanks to Khudadad for assistance in the field.

AUTHOR CONTRIBUTIONS

L.V.H. and F.M. were responsible for field collections and specimen sampling, W.E.S., L.V.H. & F.M. constructed the map. W.E.S, C.M.B, J.L.M., C.v.S., E.L., J.E. A.M., C.H.W., D.J.B. & J.R.L contributed to palaeoecological and geological interpretation. J.L.M, J.R.L, D.J.B organized and oversaw drilling operations, W.E.S. led writing of the paper with substantial contributions from C.M.B and J.L.M.

DECLARATION OF INTERESTS

The authors declare no competing interests.

REFERENCES

- Shugart, H. H., Saatchi, S. & Hall, F. G. (2010). Importance of structure and its measurement in quantifying function of forest ecosystems. *J Geophys. Res.* *115*, G00E13, doi:10.1029/2009JG000993.
- Greb, S. F., DiMichele, W. A. & Gastaldo, R. A. (2006). Evolution and importance of wetlands in earth history. *Geol. Soc. Am. Special Papers* *399*, 1–40.
- DiMichele, W. A. & Falcon-Lang, H. J. (2011). Pennsylvanian “fossil forests” in growth position (T0 assemblages): origin, taphonomic bias and palaeoecological insights. *J. Geol. Soc. (London)* *168*, 585–605.
- Meyer-Berthaud, B. & Soria A, Decombeix, A-L. (2010). The land plant cover in the Devonian: a reassessment of the evolution of the tree habit. *Geol. Soc. London Spec. Publ.* *339*, 59–70.
- DiMichele, W. A., Falcon-Lang, H. J., Nelson, W. J., Elrick, S. D. & Ames, P. R. (2007). Ecological gradients within a Pennsylvanian mire forest. *Geology* *35*, 415–418.
- Wang, J., Pfefferkorn, H. W., Zhang, Y. & Feng, Z. (2012). Permian vegetational Pompeii from Inner Mongolia and its implications for landscape palaeoecology and palaeobiogeography of Cathaysia. *Proc. Natl. Acad. Sci. USA* *109*, 4927–4932.
- Goldring, W. (1924). The Upper Devonian forest of seed ferns in eastern New York. *N.Y. State Mus. Bull.* *251*, 50-72.
- Stein, W. E., Mannolini, F., Hernick, L. V., Landing, E. & Berry, C. M. (2007). Giant cladoxylopsid trees resolve the enigma of the Earth’s earliest forest stumps at Gilboa. *Nature* *446*, 904–907.
- Stein, W. E., Berry, C. M., Hernick, L. V. & Mannolini, F. (2012). Surprisingly complex community discovered in the mid-Devonian fossil forest at Gilboa. *Nature* *483*, 78-81.

- 400 10. Retallack, G. J. & Huang, C. (2011). Ecology and evolution of Devonian trees in New York,
401 USA. *Palaeogeogr. Palaeoclimatol. Palaeoecol.* 299, 110–128.
- 402 11. Algeo, T. J. & Scheckler, S. E. (1998). Terrestrial-marine teleconnections in the Devonian:
403 links between the evolution of land plants, weathering processes, and marine anoxic events.
404 *Philos. Trans. (London) Biol. Sci.* 353B, 113-130.
- 405 12. Meyer-Berthaud, B., Scheckler, S. E. & Bousquet J-L. (2000). The Development of
406 *Archaeopteris*: New Evolutionary Characters from the Structural Analysis of an Early
407 Famennian Trunk from Southeast Morocco. *Am. J. Bot.* 87, 456-468.
- 408 13. Meyer-Berthaud, B., Decombeix, A-L. & Ermacora, X. (2013). Archaeopterid Root Anatomy
409 and Architecture: New Information from Permineralized Specimens of Famennian Age from
410 Anti-Atlas (Morocco). *Int. J. Plant Sci.* 174, 364–381.
- 411 14. Marshall, J. E. A. (1996). *Rhabdosporites langii*, *Geminospora lemurata* and *Contagisporites*
412 *optimus*: an origin for heterospory within the progymnosperms. *Rev. Palaeobot. Palynol.* 93,
413 159–189.
- 414 15. Berry, C. M. & Fairon-Demaret, M. (2001). Middle Devonian flora revisited. In *Plants*
415 *Invade the Land: Evolutionary and Environmental Perspectives* P. G. Gensel & D. Edwards,
416 eds. (New York: Columbia Univ. Press), pp. 120-139
- 417 16. Beck, C. B. (1962). Reconstructions of *Archaeopteris*, and Further Consideration of its
418 Phylogenetic Position. *Amer. Jour. Bot.* 49, 373-382.
- 419 17. Beck, C. B. (1970). The appearance of gymnospermous structure. *Biol. Rev.* 45, 379–399.
- 420 18. Brett, C.E. & Baird, G.C. (1994). Depositional sequences, cycles, and foreland basin
421 dynamics in the late Middle Devonian (Givetian) of the Genesee Valley and western Finger
422 Lakes region. In *Field trip guidebook*, C.E. Brett & J. Scatterday, eds. (New York State
423 Geological Association 66th Annual Meeting, Rochester), pp. 505-585.
- 424 19. Brett, C. E., Baird, G. C., Bartholomew, A., DeSantis, M. K., & Ver Straeten, C. A. (2011).
425 Sequence stratigraphy and revised sea level curve for the Middle Devonian in eastern North
426 America. *Palaeogeography, Palaeoclimatology, Palaeoecology*, 304, 21-53.
- 427 20. Becker, R. T., Gradstein, F. M., & Hammer, O. (2012). The Devonian Period, In *The*
428 *Geologic Time Scale 2012*, F. M. Gradstein, J. G. Ogg, M. D. Schmitz, & G. M. Ogg eds.
429 (New York: Elsevier), pp. 559-601.
- 430 21. Matten, L. C. (1968). *Actinoxylon banksii* gen. et sp. nov.: A progymnosperm from the
431 Middle Devonian of New York. *Am. J. Bot.* 55, 773–782.
- 432 22. Matten, L. C. (1975). Additions to the Givetian Cairo flora from eastern New York. *Bull.*
433 *Torrey Bot. Club* 102, 45–52.
- 434 23. Hernick, L.V., Landing, E. & Bartowski, K. E. (2008). Earth’s oldest liverworts—

- 435 *Metzgeriothallus sharonae* sp. nov. from the Middle Devonian (Givetian) of eastern New
436 York, USA. *Rev. Palaeobot. Palynol.* 148, 154–162.
- 437 24. Potvin-Leduc, D. (2015). Middle Devonian (Givetian) sharks from Cairo, New York (USA):
438 Evidence of early cosmopolitanism. *Acta. Palaeontol Pol.* 60, 183-200.
- 439 25. Soil Survey Staff (1999). *Soil Taxonomy: A basic system of soil classification for making*
440 *and interpreting soil surveys* (Natural Resources Conservation Service, U.S. Department of
441 Agriculture Handbook, 2nd ed.).
- 442 26. Retallack, G. J. (2001). Soil classification. In *Soils of the past: an introduction to*
443 *palaeopedology* (Malden, MA:Wiley-Blackwell 2nd ed), pp. 63-76.
- 444 27. Wilding, L. P. & Tessier, D. (1988). Genesis of vertisols: shrink-swell phenomena. In
445 *Vertisols: Their Distribution, Properties, Classification, and Management*, L.P. Wilding & R.
446 Puentes, eds. (College Station, TX: A&M University Printing Center), pp. 55-79.
- 447 28. Meyer-Berthaud, B., Scheckler, S.E. and Bousquet J-L. (2000). The development of
448 *Archaeopteris*: New evolutionary characters from the structural analysis of an early
449 Famennian trunk from Southeast Morocco. *Amer. J. Bot.* 87, 456-468.
- 450 29. Mintz, J.S, Driese, S.G. and White J.D. (2010). Environmental and ecological variability of
451 Middle Devonian (Givetian) forests in Appalachian basin paleosols, New York, United
452 States. *Palaaios* 25, 85-96.
- 453 30. Bridge, J.S. (2000). The geometry, flow patterns and sedimentary processes of Devonian
454 rivers and coasts, New York and Pennsylvania, USA. *Geol. Soc. London Special Publication*
455 180, 85–108.
- 456 31. Driese, S.G., Mora, C.I. and Elick, J.M. (1997). Morphology and taphonomy of root and
457 stump casts of the earliest trees (Middle to Late Devonian), Pennsylvania and New York,
458 U.S.A. *Palaaios* 12, 524-537.
- 459 32. Bridge, J.S. and Willis, B. (1994). Marine transgressions and regressions recorded in Middle
460 Devonian shore-zone deposits of the Catskill clastic wedge. *Geol. Soc. Am. Bull.* 106, 1440-
461 1458.
- 462 33. Dorning, K.J. (1987). The organic palaeontology of Palaeozoic carbonate environments. In
463 *Micropalaeontology of carbonate environments*, M.B Hart, ed. (Chichester, UK: Ellis
464 Horwood & British Micropalaeontology Society Series), pp. 256-265.
- 465 34. Colbath, G.K. and Grenfell, H.R. (1995). Review of biological affinities of Palaeozoic acid-
466 resistant, organic walled eukaryotic algal microfossils (including “acritarchs”). *Rev.*
467 *Palaeobot. Palynol.* 86, 287-314.
- 468 35. Xu, H-H. et al. (2017). Unique growth strategy in the Earth’s first trees revealed in silicified
469 fossil trunks from China. *Proc. Natl. Acad. Sci. USA* 114, 12009-12014.

- 470 36. Wight, D.C. and Beck, C.B. (1984). Sieve cells in phloem of a Middle Devonian
471 progymnosperm: *Science* 225, 1469-1471.
- 472 37. Stein, W.E. and Beck, C.B. (1983). *Triloboxylon arnoldii* from the Middle Devonian of
473 western New York. *Contr. Mus. Paleont. Univ. Mich.* 26, 257-288.
- 474 38. Dannenhoffer, J.M., Stein, W.E. and Bonamo, P.M. (2007). The primary body of *Rellimia*
475 *thomsonii*: integrated perspectives based on organically connected specimens. *Internat. J. Pl.*
476 *Sci.* 168, 491-506.
- 477 39. Grierson, J.D. and Banks, H.P. (1963). Lycopods of the Devonian of New York State:
478 *Palaeontogr. Am.* 4, 220-295.
- 479 40. Banks, H.P., Bonamo, P.M. and Grierson, J.D. (1972). *Leclercqia complexa* gen. et sp. nov.,
480 a new Lycopod from the late Middle Devonian of eastern New York. *Rev. Palaeobot.*
481 *Palynol.* 14, 19–40.
- 482 41. White, D. (1907). A remarkable fossil tree trunk from the Middle Devonian of New York.
483 *N.Y. State Mus. Ann. Rept.* 107, 327–340.
- 484 42. Berry, C.M. and Marshall, J.E.A. (2015). Lycopsid forests in the early Late Devonian
485 palaeoequatorial zone of Svalbard. *Geology* 43, 1043–1046.
- 486 43. Wang, D. et al. (2019). The most extensive Devonian fossil forest with small lycopsid trees
487 bearing the earliest stigmarian roots. *Current Biology* 29, 2604-2615.
- 488 44. Bauhus, J. & Messier, C. (1999). Soil exploitation strategies of fine roots in different tree
489 species of the southern boreal forest of eastern Canada. *Can. J. For. Res.* 29, 260–273.
- 490 45. Danjon, F. & Reubens, B. (2007). Assessing and analyzing 3D architecture of woody root
491 systems, a review of methods and applications in tree and soil stability, resource acquisition
492 and allocation. *Plant Soil* 303, 1–34.
- 493 46. Algeo, T. J, Scheckler, S. E. & Maynard, J. B. (2001). In *Plants Invade the Land:*
494 *Evolutionary and Environmental Perspectives* P. G. Gensel & D. Edwards, eds. (New York:
495 Columbia Univ. Press), pp. 213-236.
- 496 47. Gibling, M. R. & Davies, N. S. (2012). Palaeozoic landscapes shaped by plant evolution.
497 *Nature Geosci.* 5, 99–105.
- 498 48. Quirk, J., Leake, J. R., Johnson, D. A., Taylor, L.L., Saccone, L. & Beerling, D. J. (2015).
499 Constraining the role of early land plants in Palaeozoic weathering and global cooling. *Proc.*
500 *R. Soc. B* 282, 2015.1115, doi10.1098/rspb.2015.1115.
- 501 49. Morris, J. L. et al. (2015). Investigating trees as geo-engineers of past climates: linking
502 palaeosols to palaeobotany and experimental geobiology. *Palaeontology* 58, 787–801.
- 503 50. Ibarra, D. E. et al. (2019). Modeling the consequences of land plant evolution on silicate

504 weathering. Amer. J. Sci. 319, 1-43.

505

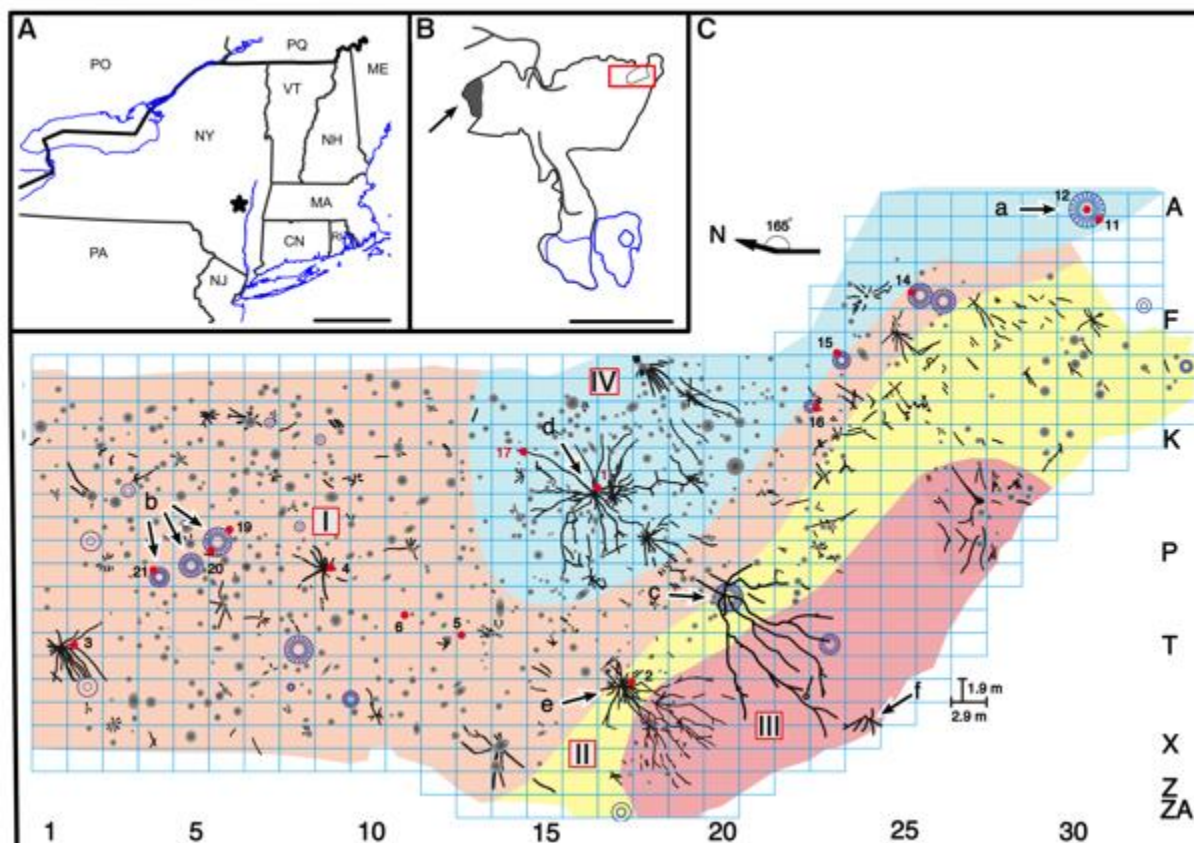
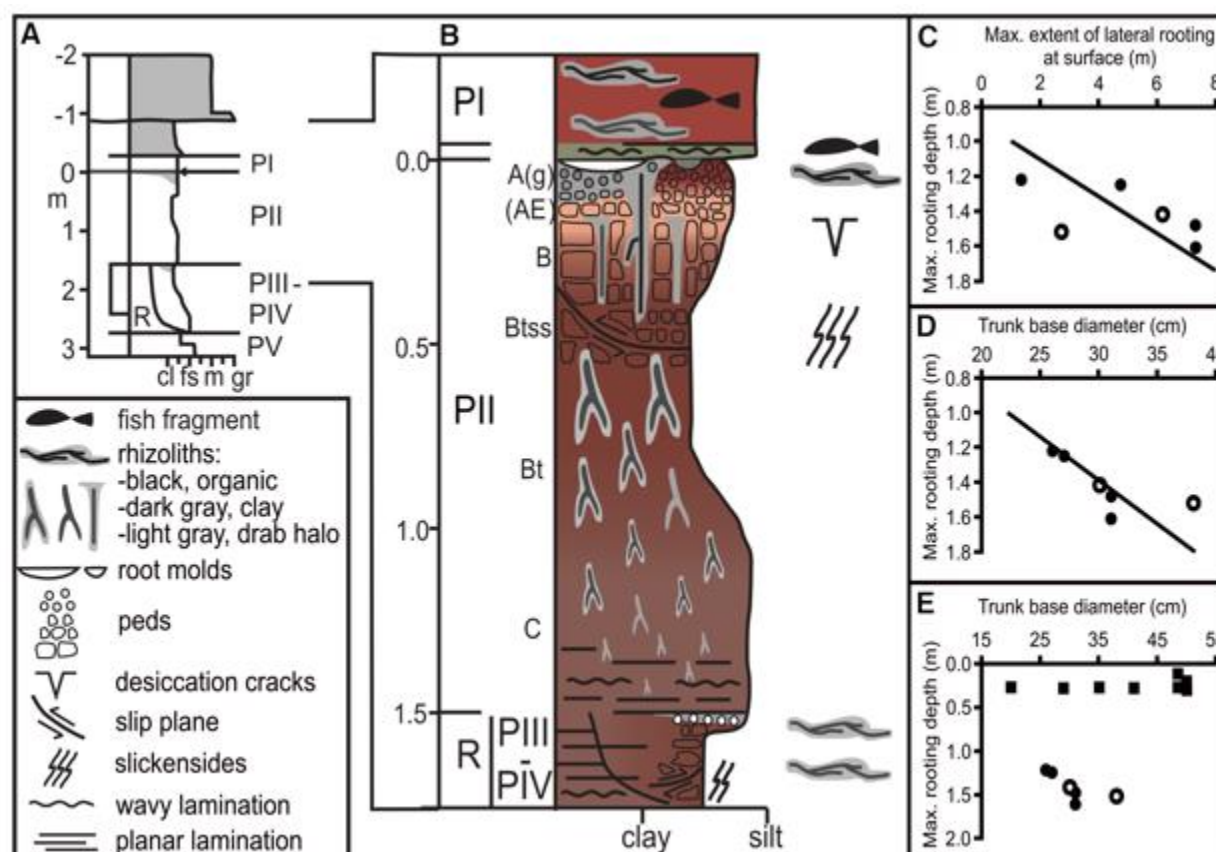


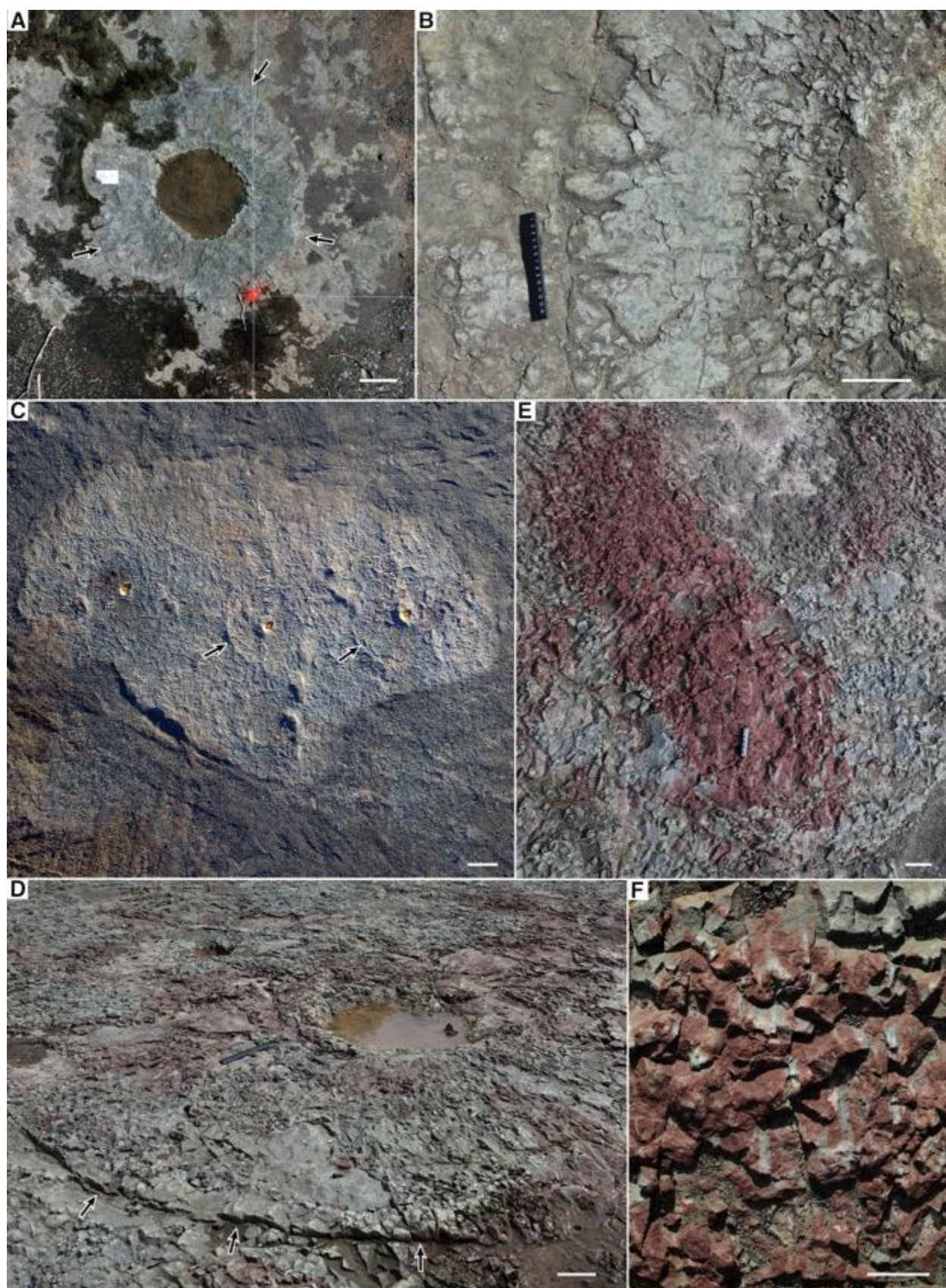
Figure 1. Location and plan map of the Cairo site.

(A) General location. Scale bar 160 km (100 mi).

(B) Cairo Quarry. Blue outlines water ponds; shaded region (arrow) dark shale; red rectangle mapped region. Scale bar, 213 m (700 ft).

(C) Plan map. Color-shaded regions I-IV indicate approximate extent of differing surface features of paleosol PII in Figure 2B, and as described in the text. Identified *Eospermatopteris* root systems are indicated by blue double circles with stylized radiating lines indicating approximate radial extent of roots observed on the paleosol surface when present. Black lines indicate identified *Archaeopteris* root systems and isolated linear roots. Numbers and red circles indicate some of the cores drilled at the site (not all cores were drilled on the mapped surface). Gray shaded circles/ellipses indicate surface depressions indicating original paleosol topography or potential floral elements that could not be positively identified. Arrows indicate specific individuals also identified in other figures: a, partially cast *Eospermatopteris* (Figures 3A, 3B; Supplemental Figures 1A, 2A, 2C); b, three well-preserved *Eospermatopteris* seated directly on mottled paleosol (Figures 3C-F; Supplemental Figures 1, 2B); c, unidentified root system, potentially lycopsid, with large primary roots bearing rootlets (Figure 6; Supplemental Figures 1, 5); d, partly cast *Archaeopteris* root systems associated with vertebrate remains (Figures 4A-B; Supplemental Figure 1); e, best preserved *Archaeopteris* showing extensive articulated root system (Figures 4C, 5); f, smaller *Archaeopteris* root system preserved entirely within the limonite-stained region (Supplemental Figure. 1A).





544 **Figure 3. *Eospermatopteris* root systems**

545 (A) Individual a in [Figure 1C](#), partly cast by greenish siltstone (overwash sediment), showing
 546 deep water-filled central depression where the tree base once sat surrounded by preserved roots
 547 radiating from the center. Arrows indicate a distinct boundary in the paleosol, characterized by
 548 subvertical slickenside surfaces. Scale bar, 20 cm.

549 (B) Magnified view of radiating roots near left arrow in (A). The root mass forms an imbricate
 550 system with individual roots occurring on the surface as impressions. Scale bar, 10 cm.

551 (C) Three individuals indicated by arrows b in [Figure 1C](#) occurring on the surface of the mottled
 552 paleosol. Central depressions, marked by orange cones, surmount shallow mounds bearing
 553 numerous roots. The arrows mark paleosol boundary with slickenside surfaces. Scale bar, 50
 554 cm.

555 (D) Right-hand individual indicated by arrows b in [Figure 1C](#), showing root mound with distinct
 556 boundary, arrows, with subvertical slickenside surfaces. Scale bar, 10 cm.

557 (E) Magnified portion of root mound of left-most individual indicated by arrows b in [Figure 1C](#).
 558 Center of root system is toward the top of the image with roots showing reduced halos. Scale bar,
 559 5 cm.

560 (F) Magnified view of root halos in (E). Scale bar, 3 cm.

561

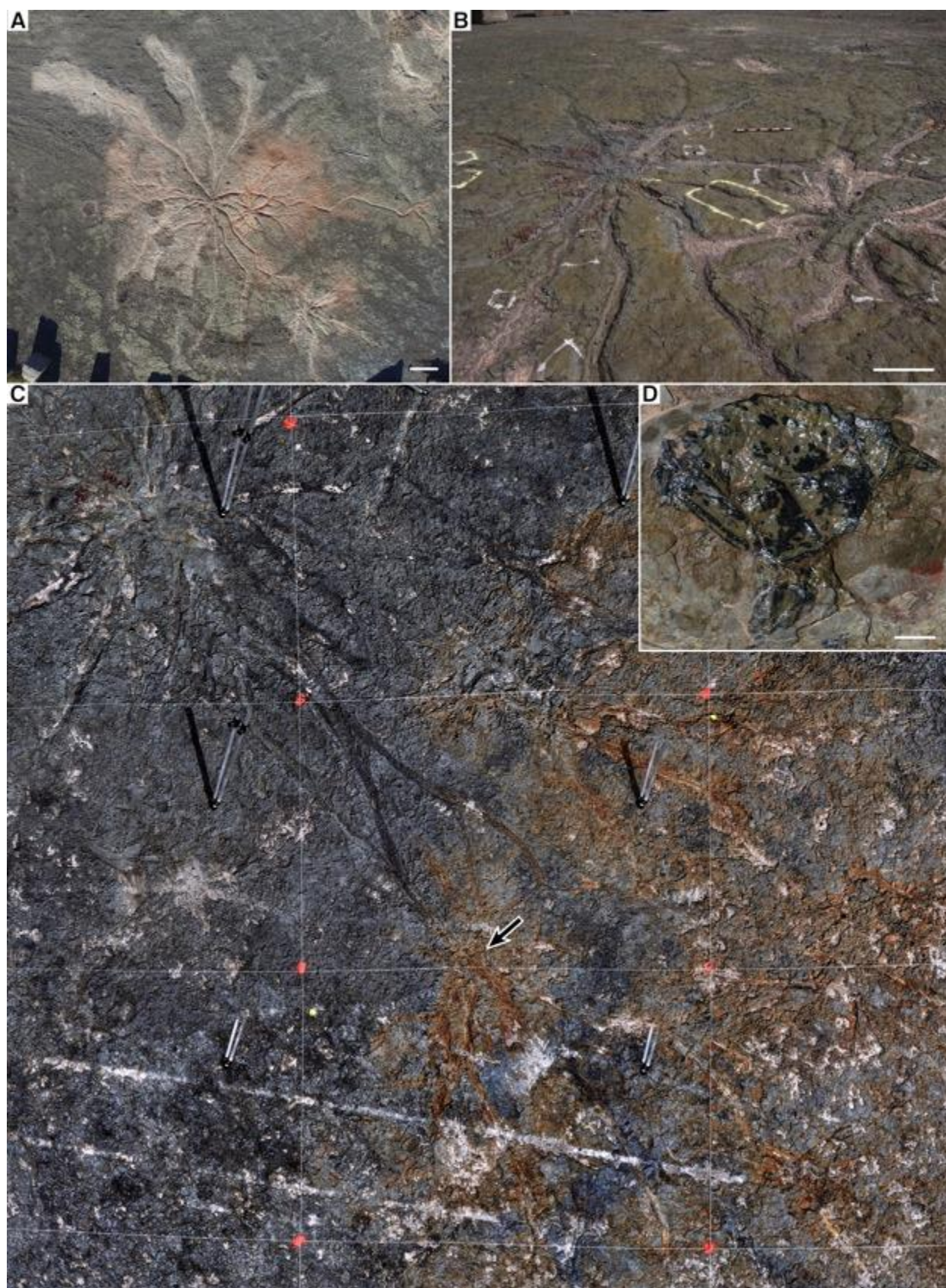


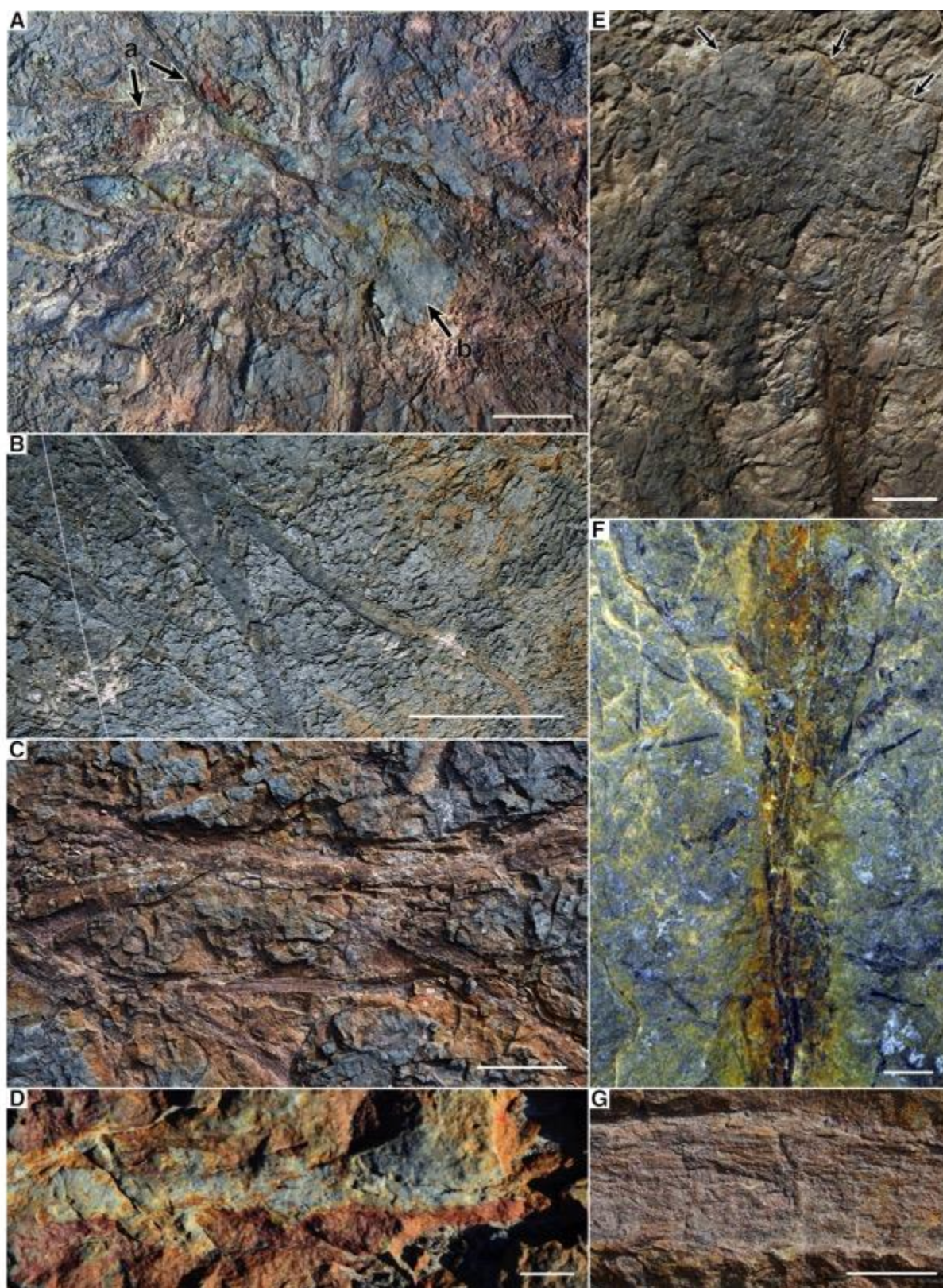
Figure 4. *Archaeopteris* Root systems

(A) Aerial view of a conspicuous pair of bases partly cast by greenish overwash siltstone (region IV), indicated by arrow d in [Figure 1C](#). Scale bar, 1 m.

(B) Same pair with only the largest structural roots seen on the surface and reddish surface mottling near root system centers. Yellow polygons on the paleosol indicate fish remains. Scale bar, 50 cm.

(C) Stitched view from 6 photographs of best-preserved individual showing its highly ramified root system, indicated by arrow e in [Figure 1C](#). Center of root system is at upper left. Primary structural roots trend mostly to the southwest in organic connection throughout most of this view. Roots are dark impressions in the dark gray palaeosol region ([Figure 1C, region II](#)), becoming increasingly encrusted with limonite toward and into the limonite stained palaeosol region ([Figure 1C, region III](#)). Arrow indicates possible root clone individual. The 1.9 X 2.9m map grid with red paint intersections provides scale.

(D) Vertebrate (fish) fossil shown here as example of multiple specimens found on the surface of the overwash sediment ([Figure 1C, region IV](#)). Scale bar, 2 cm.



580 **Figure 5. Details of *Archaeopteris* individual in Figure 4C.**

581 (A) Center of root system showing complex branching of primary structural roots, red palaeosol
582 pushed up from below at arrows a, and isolated patch of overwash siltstone at arrow b. Scale bar,
583 20 cm.

584 (B) Region near center of Figure 4C showing more-or-less equal dichotomies of some of the
585 largest structural roots. Scale bar, 50 cm.

586 (C) Unequal branching of structural roots ca. 3 m from the center at left. Scale bar, 10 cm.

587 (D) Detail of smallest scale structural roots apparently giving off multiple rootlets. Scale bar, 1
588 cm.

589 (E) Primary structural root near termination, distal end up. Arrows mark boundary with
590 slickensides between root-bound and non-bound palaeosol. Scale bar, 10 cm.

591 (F) Small root showing attached and associated finest-scale rootlets, photographed at night with
592 cross-polar light. Scale bar, 1 cm.

593 (G) Detail of distal root with limonite-filled transverse cracks. Scale bar, 1 cm.

594

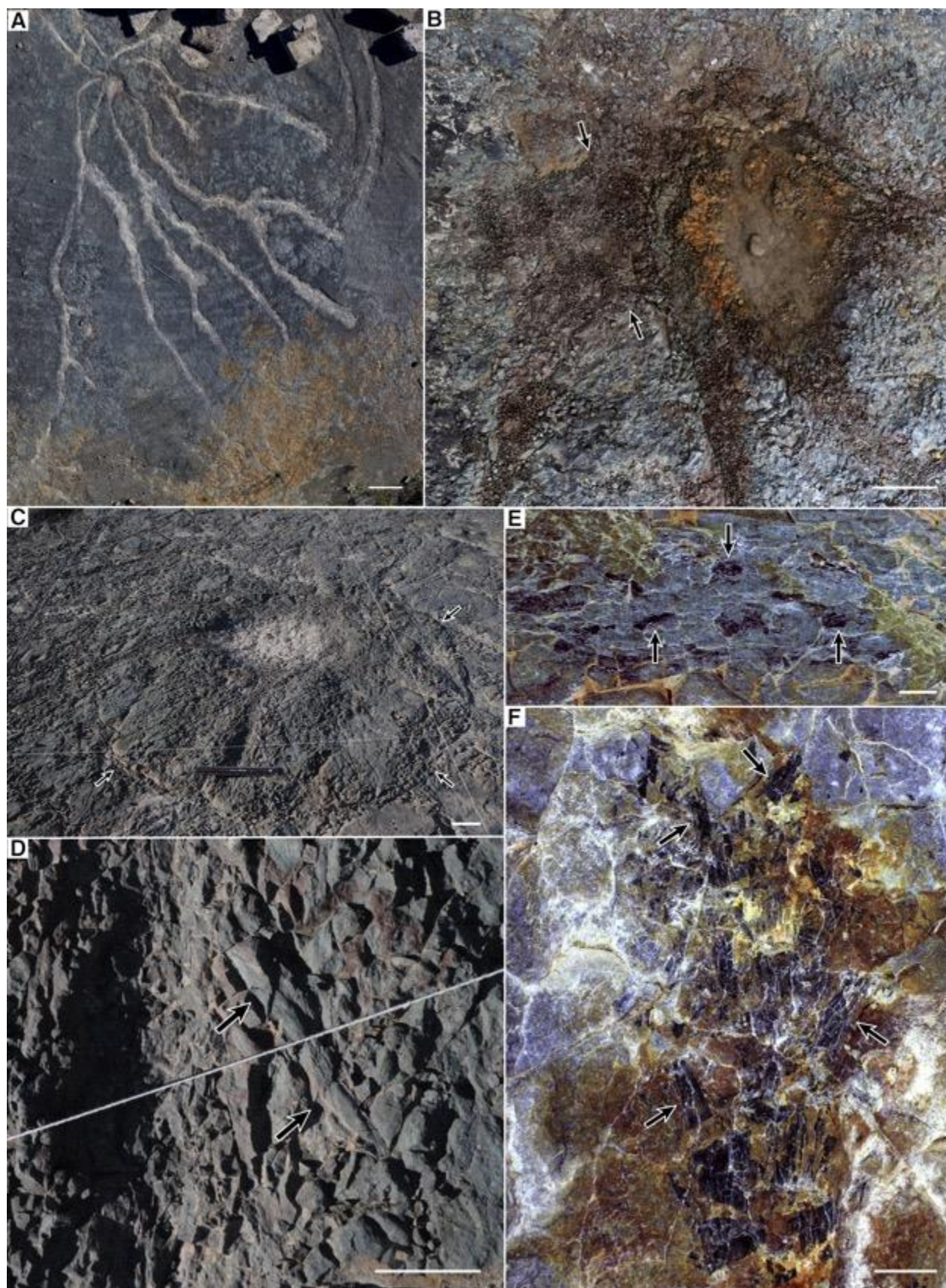


Figure 6. Root system, potentially lycopsid, showing large primary roots with radiating rootlets, indicated by arrow c in Figure 1C.

(A) Aerial view showing root system center upper left, with sparsely dichotomous primary roots, trending toward the limonite stained region at lower right. Scale bar, 1 m.

(B) Center of root system, wet, with limonite incrustated center, and red-stained primary roots. Arrows indicate lateral limit of the largest primary root that appears bifurcate at or near attachment to the base. Scale bar, 20 cm.

(C) Root system, dry, showing root mound in oblique view. Arrows indicate nearly circular boundary with subvertical slickensides. Scale bar, 10 cm.

(D) Magnification of root spanned by ruler in C, with attached lateral rootlet, one of several, indicated by arrows. Scale bar, 5 cm.

(E) Secondary root approximately midway between center and observed tip, at night in cross-polar light. Arrows indicate black carbon flecks in regular array likely at attachment points of lateral rootlets. Scale bar, 1 cm.

(F) Secondary root at or near terminus in cross-polar light, distal end up. Remnants of rootlets with fine longitudinal striations appear to diverge distally outward, indicating attachment and better preservation near the root tip. Scale bar, 1 cm.

STAR*METHODS

KEY RESOURCES TABLE

LEAD CONTACT AND MATERIALS AVAILABILITY

Requests for further information should be directed to Corresponding Authors, William Stein (stein@binghamton.edu), Chris Berry (berryCM@cardiff.ac.uk), or Jennifer Morris (drjenlmorris@gmail.com). Access to materials should be directed to the New York State Museum or Cardiff University.

Cairo Quarry and Materials

The large Cairo quarry ([Figure 1B](#)) comprises multiple loci of excavation at different topographic levels, but local faulting restricts interpretation of the stratigraphic correlation between exposures within the site. Quarry walls show 1-3 stacked sets of low-angle cross-bedded sandstones, whereas lower excavations expose thinly bedded fine-grained siltstones associated with multiple inter-bedded shale and paleosol horizons. In one part of the quarry, a ca. 1.5 m thick dark weakly fissile shale yields conchostrachans and plant debris and is tentatively interpreted by us as remains of a fresh-water lake ([Figure 1B, arrow](#)). Access to this site is by permission only.

The Cairo quarry occurs approximately 122-152m below the base of the Manorkill Formation [1], and roughly in the middle of the Plattekill Formation, which is estimated to have a maximum thickness of ca. 305m at the Catskill Front [2]. The boundary between the Plattekill and Manorkill Formations in the study area is a chronostratigraphic boundary, marked by a same-age conglomerate event bed, which correlates with a basal sandstone to limestone of the marine Moscow Formation in central to western New York State. By contrast, the Riverside quarry at Gilboa occurs either in strata correlative with the lower Moscow Formation (locally the lower part of the nearshore Cooperstown Formation) [3,4] or in the upper lower to middle part of the Cooperstown Formation in the Schoharie Valley (upper part of the fourth of seven Moscow subsequences, correlative with a unit called the Bear Swamp Beds) [5]. At this time the viability of Rickard's versus Bartholomew's correlations of the Riverside Quarry is unclear. Nevertheless, the Cairo Quarry is definitely older than the Riverside quarry at Gilboa.

Based on sequence stratigraphic analyses of the Middle Devonian Hamilton Group, and estimated duration of Milankovitch cyclicity in the Givetian Stage, a 1.8 Ma duration for the Ludlowville Formation, and 1.2 Ma duration for the lower to middle Moscow Formation up through the Bear Swamp Beds has been estimated, giving a total duration of ca. 7.5 Ma for the stage [6]. If, as presented above, the Cairo quarry occurs in mid-Plattekill position correlative with the base of the marine Ludlowville Formation to the west, and the Riverside Quarry occurs in mid-Moscow strata correlative with the Bear Swamp Beds, then the time span between deposition of the Cairo quarry and Riverside quarry forests would approximate 3 Ma. However, another recent Devonian time scale estimates only 5.0 Ma for the Givetian Stage [7]. This and lack of clarity on exact stratigraphic correlations may shorten the estimated time between the Cairo and Gilboa forests to approximately 2 Ma.

Surface samples have been taken for laboratory study. In addition, 7.6 cm (3-inch) cores (numbered 1-6 in 2012 and 11-22 in 2013) were drilled across and beyond mapped area to depths ranging between 1 to 3 m (Figure 1C). In all cases, care was exercised to leave important features of root systems and the entire site relatively intact for further *in situ* study and potential conservation by local authorities. All surface collections now belong to the New York State Museum (NYSM) in Albany NY. The cores were cut in half longitudinally, with half conserved at the NYSM, the other half sampled for further study at the University of Sheffield and National Oceanography Center, Southampton, and now permanently housed at Cardiff University, UK.

METHOD DETAILS

When originally discovered in 2009, some root systems were partly revealed on a hard surface with regularly arrayed blast fractures exposed by quarrying operations some 40+ years earlier. Careful uncovering of loose fragments and exogenous gravel was performed in stages followed by laying down a grid system with individual blocks measuring 1.9m by 2.9m for complete photographic coverage (Figure 1C). A photographic record of the surface was then made at grid intersection points using a specially constructed 4m tripod, boom, digital camera and lens covering the grid system with sufficient overlap. When a drone became available, portions of the site were uncovered again and photographed at varying heights (Figures 3C, 4A, 6A; Supplemental Figures S1, S3A). Root systems were imaged both dry and wet during the day, taking advantage of natural light at different angles to emphasize features. Other details were photographed at night using cross-polar light (Figure 5F, 6E-F).

Measurements

Individual root base locations may be identified using the 2.9m x 1.9m grid system with grid rows given consecutive letters A-Z + ZA and grid columns numbered 1-33 (Figure 1C). Two tree bases assignable to *Eospermatopteris* occur within grid E26, and provide the only instance of ambiguity. These are further labeled in the table as E26a for the left-hand base, and E26b for the right-hand base in the tables respectively.

Eospermatopteris - Individuals offer differing certainty depending on what was observed in the field (see downloadable [datafile](#)). As a result, they are broadly classified as C for “certain”, versus Cp for “possible or probable” as done previously at Riverside Quarry, Gilboa. Where considered meaningful, measurements were collected of the central depression in the palaeosol made by the plant base (D), with minimum (Da) and maximum (Db) values indicating major and minor axes of an ellipse circumscribing the depression respectively. In well-preserved examples, the floor of the central depression rises outward to a circular to elliptical ridge, presumably representing upward displacement of the palaeosol by trunk weight and growth. Dimensions across the ridges have also been measured (R), using minimum (Ra) and maximum (Rb) values, and provides a different assessment of plant base size. In addition, the surrounding root masses observed on the palaeosol surface were measured (S), with minimum (Sa) and maximum (Sb) values in cases where preservation permitted potentially useful data. Specific features observed in each case are indicated by columns a-d (with features defined in the dataset), where 0 = not observed, and 1 = observed.

Archaeopteris - All curvilinear structures that are likely roots are shown in black on the map (Figure 1C). Among the best candidates for assignment to *Archaeopteris* are those identified by unique number, grid location, and trunk base diameters (ID, Loc, and TBD in [datafile](#)). However, determining exact boundaries between trunk base and the largest lateral roots is imprecise due to minimal preservation of details in the palaeosol directly relating to the trunk above. Potentially more precise measurements include diameters of lateral roots (LR) and maximum observed diameters of lateral roots (LRD) (also in the [datafile](#)). Although the data points are few, a positive relationship is seen between measured trunk base diameter TBD and LRD ([Supplemental Figure S6B](#)).

Estimating *Archaeopteris* Tree Sizes at Cairo

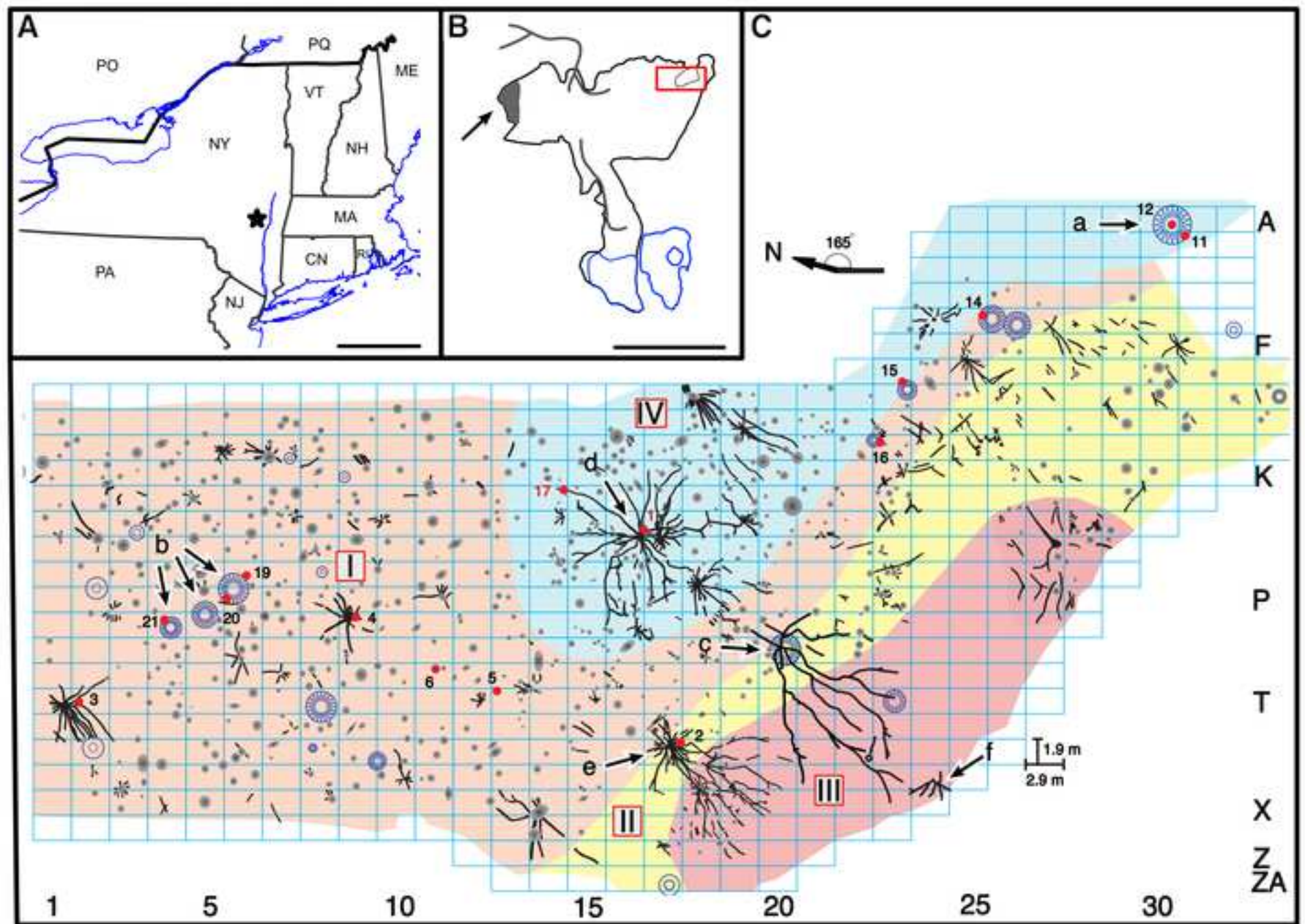
Although the field of plant allometry is large, we have not found directly applicable equations relating variables we can measure from the paleosol surface with diameter of the main trunk at breast height (DBH) commonly encountered in allometric studies, or overall tree height. So here we take a different approach. It is widely assumed that *Archaeopteris* trees more-or-less followed the tapered form seen today among conifers [8], and probably most seed plants, given shared presence of secondary growth. If so, then diameter of the largest roots (LRD) likely has a direct relationship with diameter at breast height (DBH), and from the DBH tree heights can be estimated using published regression parameters. To see whether a relationship might be found in a modern primitive conifer, data comprising LRD observed on a modern soil surface and DBH were collected in 2010 in a pilot dataset for *Araucaria* growing in domestication on the island of O'ahu, Hawaii ([see datafile](#)). A positive relationship is seen ([Supplemental Figure S6A](#)), supporting use of LRD as a proxy for DBH. Using simple linear (LM) and reduced major axis (RMA) [9] regression parameters from *Araucaria*, estimates of DBH derived from LRD for the Cairo *Archaeopteris* trees were then calculated. These estimates of DBH for *Archaeopteris* were then used to estimate *Archaeopteris* tree height using a very simple power function for conifers [10]: $H = a \cdot \text{DBH}^b$, $a=3.21$, $b=0.6$, where H is in m, DBH in cm. In addition, since *Archaeopteris* trunk base diameters (TBD) measured in the field also show a positive relationship with LRD ([Supplemental Figure S6B](#)), tree heights were estimated directly from *Archaeopteris* TBD using the same conifer formula, but here ignoring taper. Analysis was carried out using Microsoft Excel and the R Statistical computing platform. All height estimates ([Supplemental Table S1](#)) indicate trees of moderate sizes. However, all estimates should only be considered approximations primarily designed to illustrate the approach taken.

References

1. Rickard, L. V. (1968a). Bedrock map of the Durham 15' Quadrangle. New York State Museum, Geology Open Files, no. 1g1040.
2. Fletcher, F. W. (1967). Middle and Upper Devonian clastics of the Catskill front, New York. In New York State Geological Association Guidebook, R. H. Wainess ed., 39th Annual Meeting, New Paltz, pp. C1-C23.
3. Rickard, L. V. (1968b). Bedrock map of the Gilboa 15' Quadrangle. New York State Museum, Geology Open Files, no. 1g1601.

4. Rickard, L.V. (1975). Correlation of the Silurian and Devonian rocks in New York State. (Albany: University of the State of New York)
<https://nysl.ptfs.com/data/Library1/Library1/pdf/1895260.pdf>
5. Bartholomew, A.J. (2002). Correlation of High Order Cycles in the Marine-Paralic Transition of the upper Middle Devonian (Givetian) Moscow Formation, Eastern New York State. M.S. thesis, University of Cincinnati, 93 pp.
6. Brett, C. E., Baird, G. C., Bartholomew, A., DeSantis, M. K., & Ver Straeten, C. A. (2011). Sequence stratigraphy and revised sea level curve for the Middle Devonian in eastern North America. *Palaeogeography, Palaeoclimatology, Palaeoecology*, 304, 21-53.
7. Becker, R. T., Gradstein, F. M., & Hammer, O. (2012). The Devonian Period, In *The Geologic Time Scale 2012*, F. M. Gradstein, J. G. Ogg, M. D. Schmitz, & G. M. Ogg eds. (New York: Elsevier), pp. 559-601.
8. Beck, C. B. (1970). The appearance of gymnospermous structure. *Biol. Rev.* 45, 379–399.
9. Sokal, R. R. & Rohlf, J. (1994). *Biometry: The Principles and Practices of Statistics in Biological Research*. (New York: W.H. Freeman, 3rd ed.).
10. Hulshof, C. M., Swenson, N. G. & Weiser, M. D. (2015). Tree height-diameter allometry across the United States. *Ecol. Evol.* 5, 1193–1204.

[Click here to access/download;Figure;191017 CB Fig 1.tiff](#)



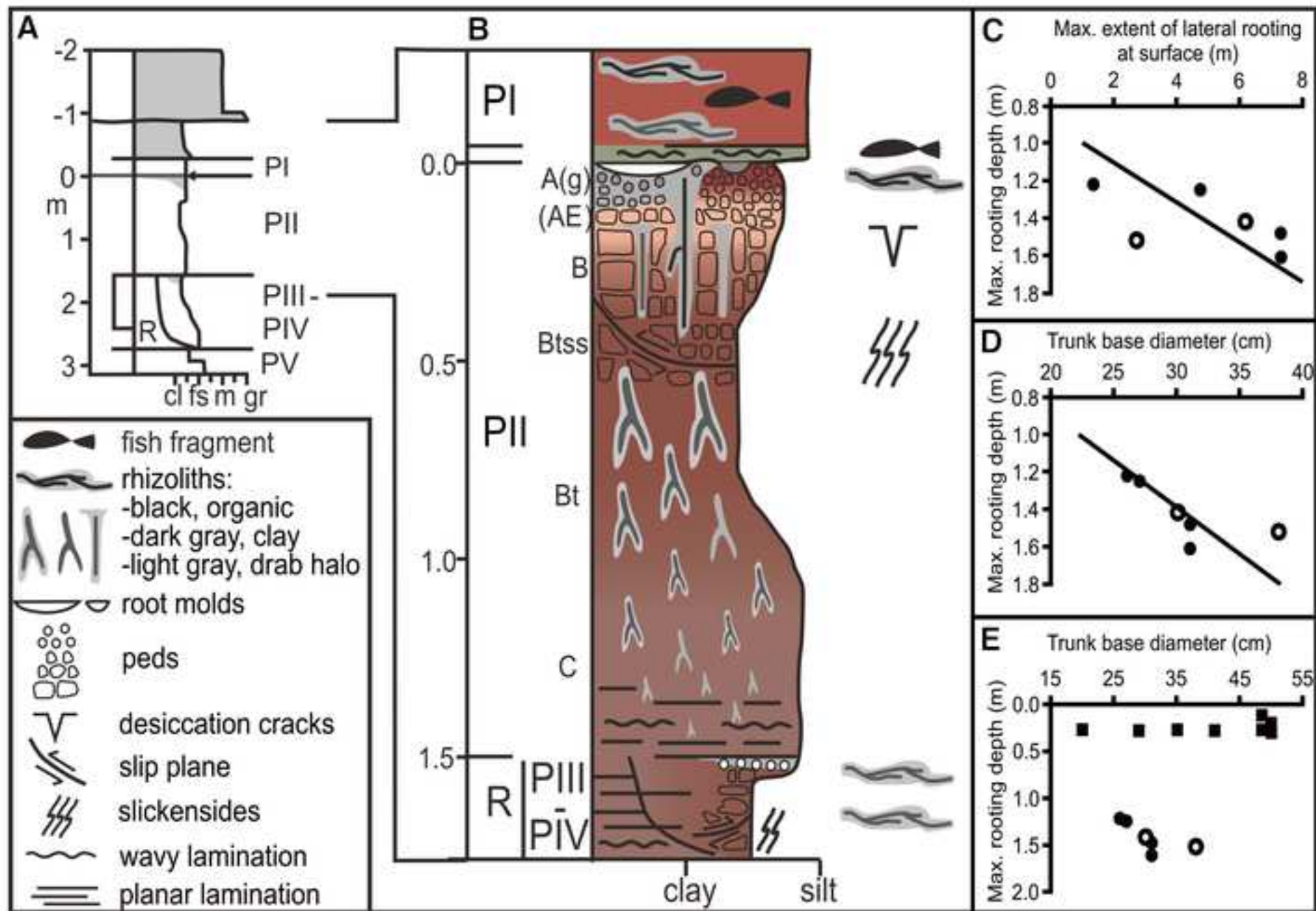




Figure 4

[Click here to access/download;Figure;191017 CB Fig 4.tiff](#) 

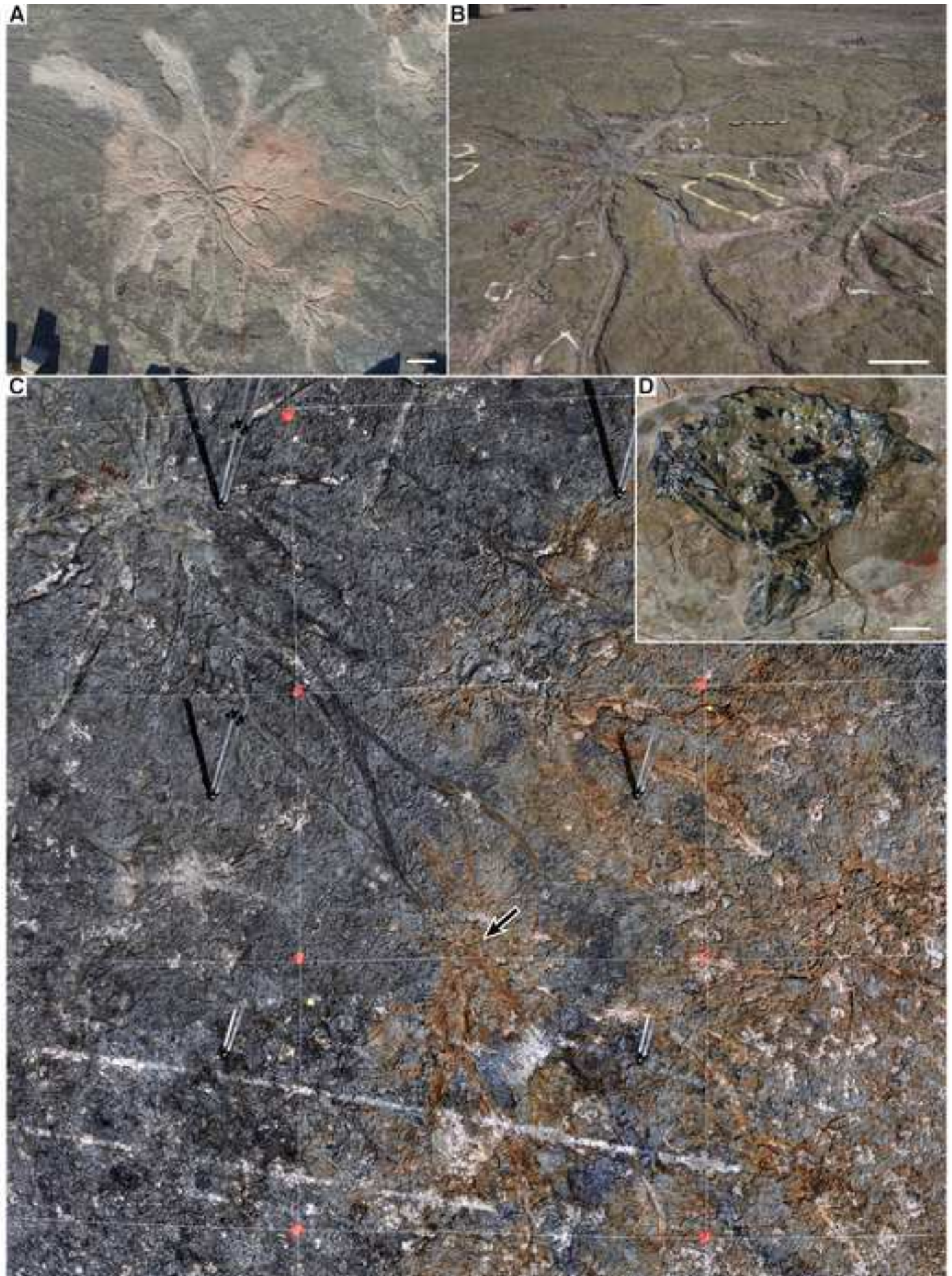


Figure 5

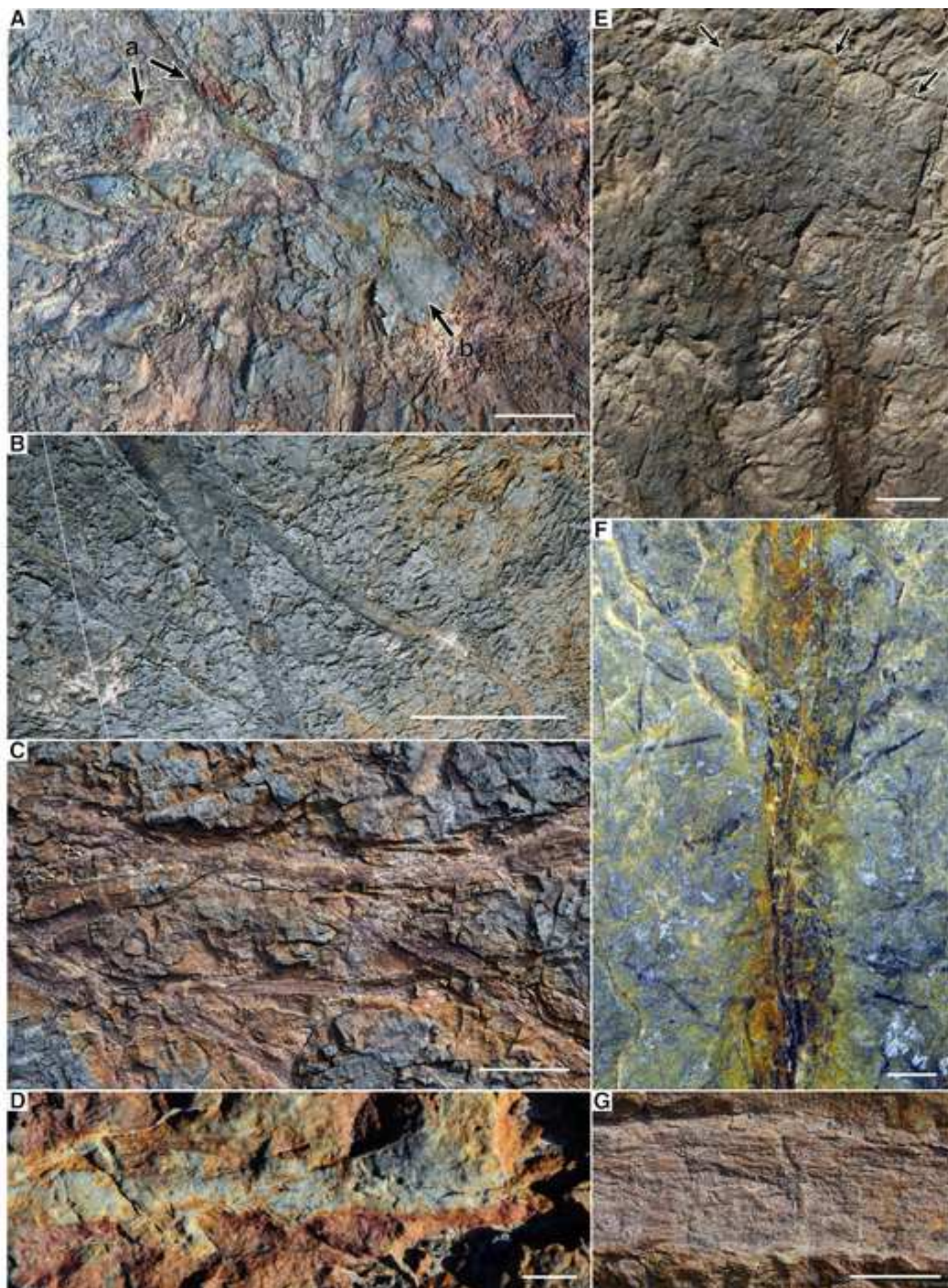
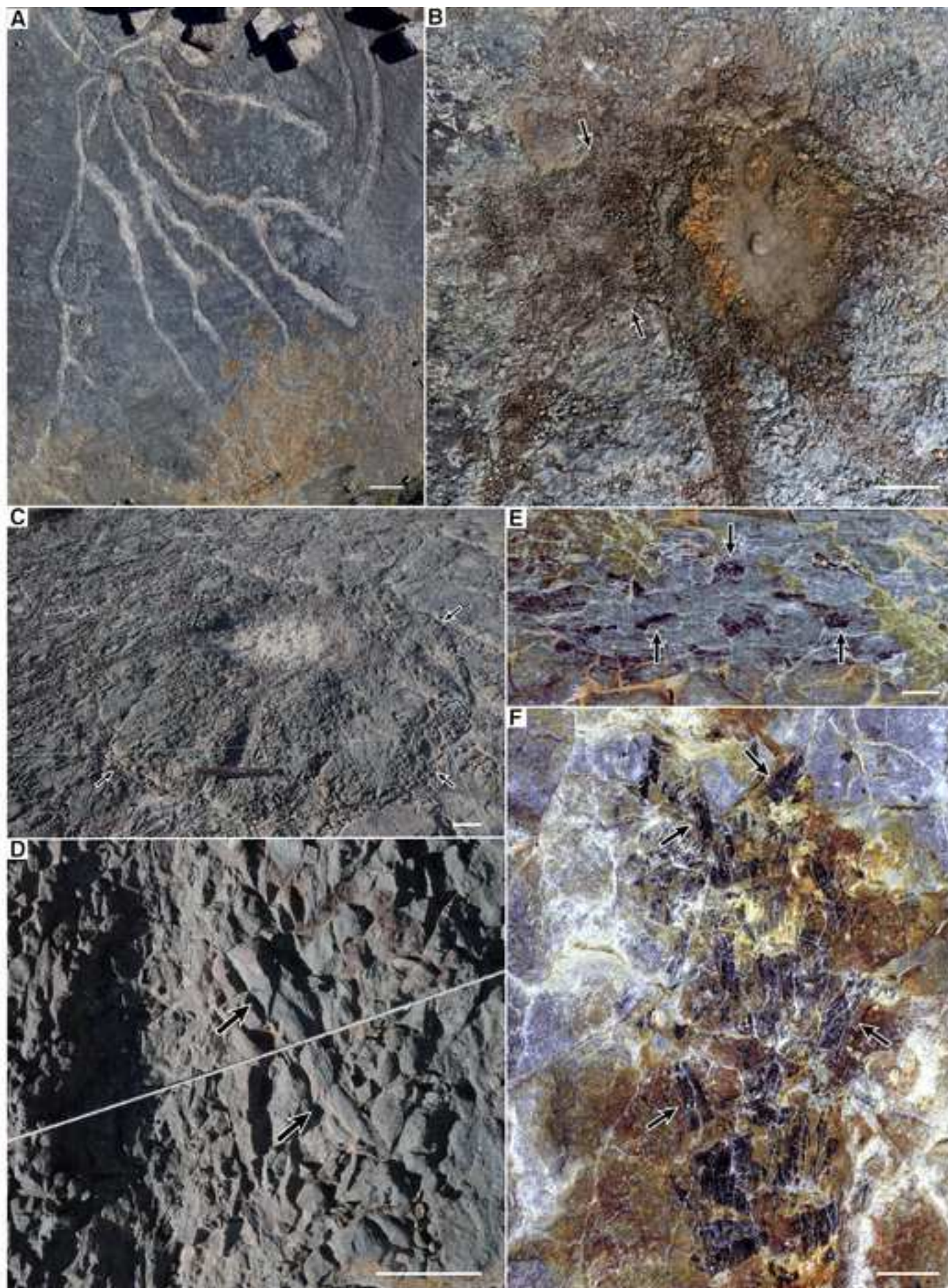
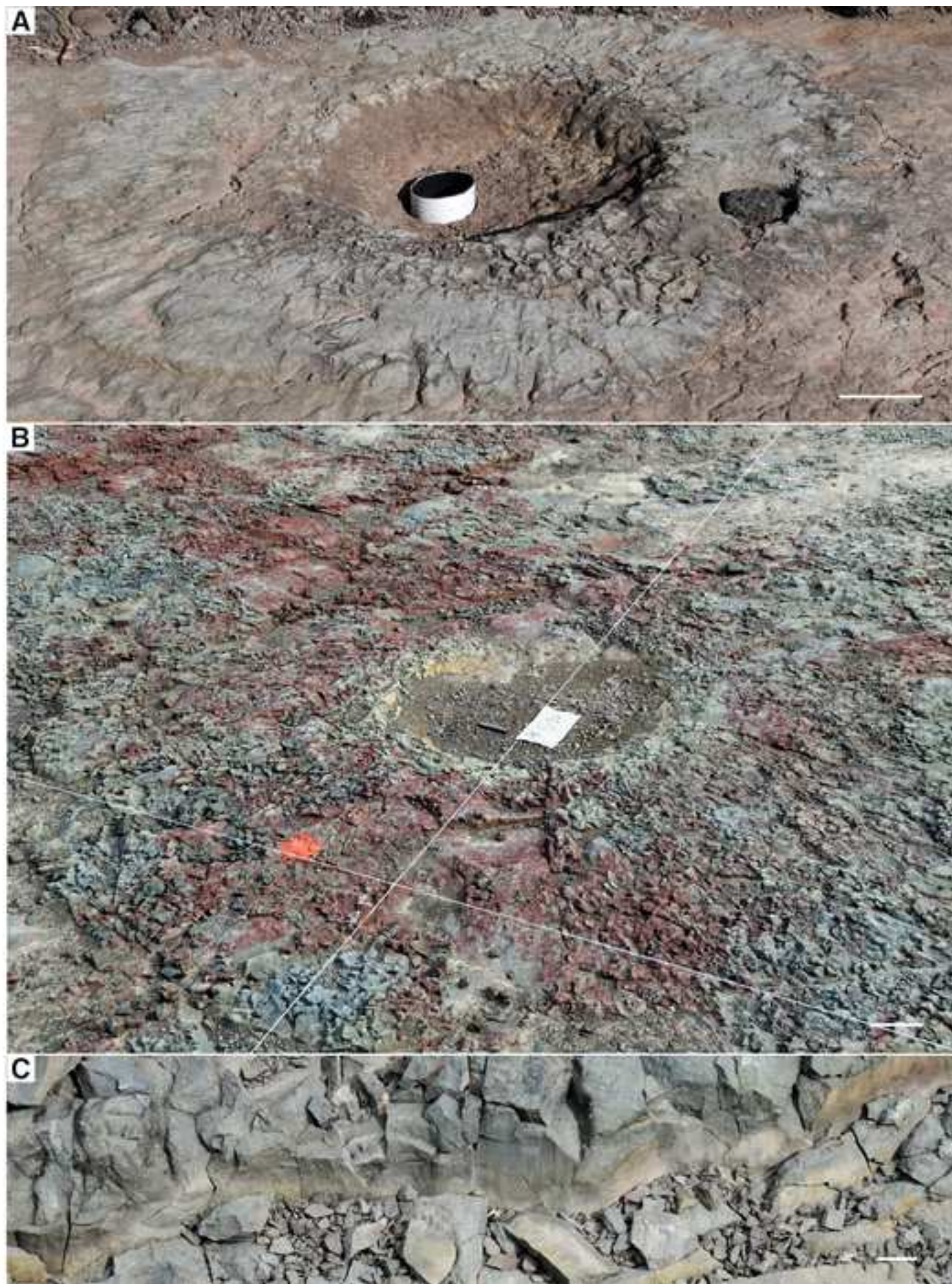


Figure 6

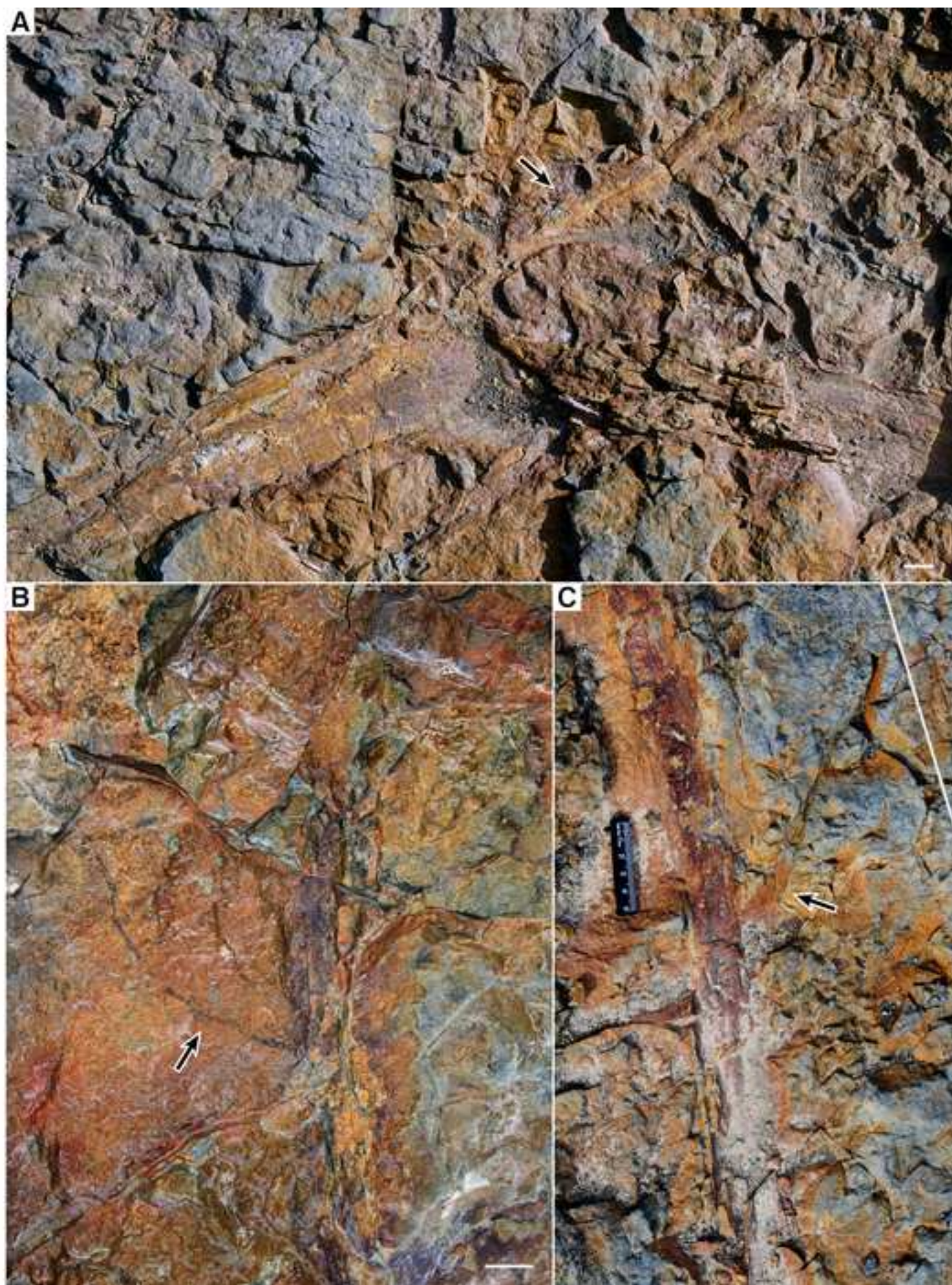
[Click here to access/download;Figure;191017 CB Fig 6.tiff](#)

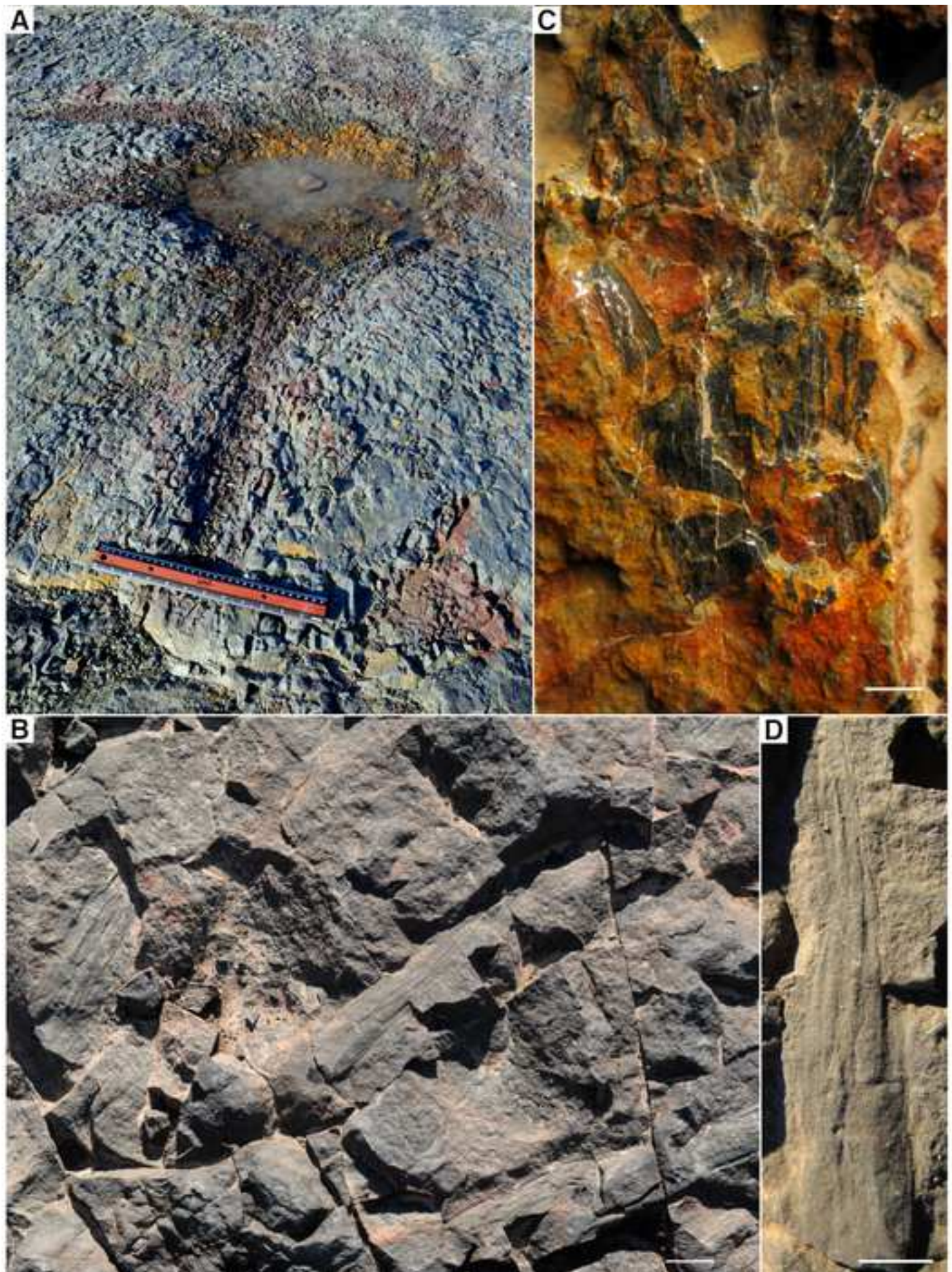












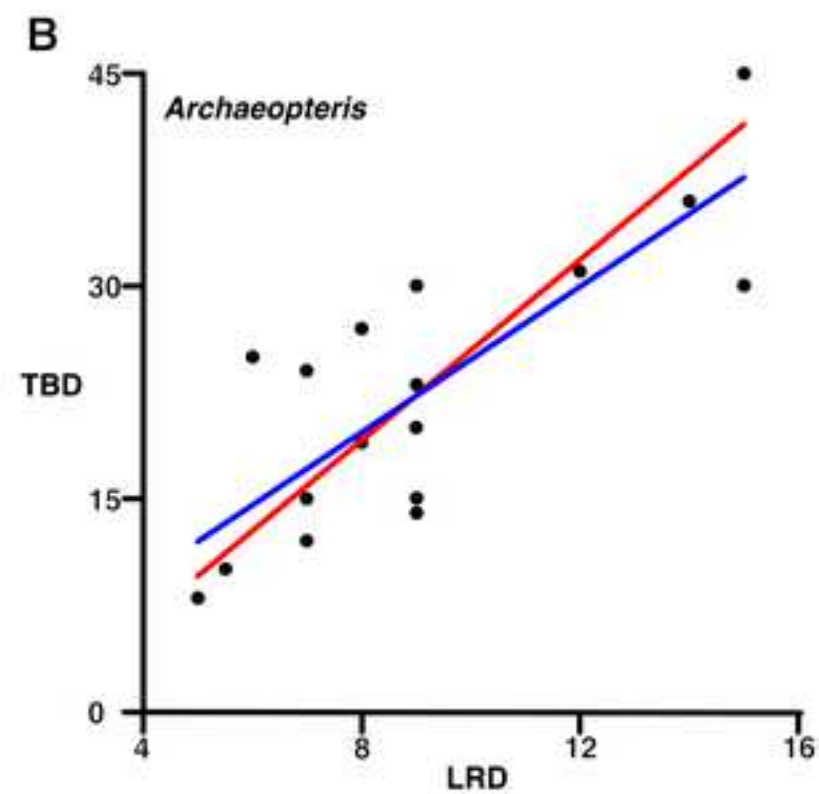
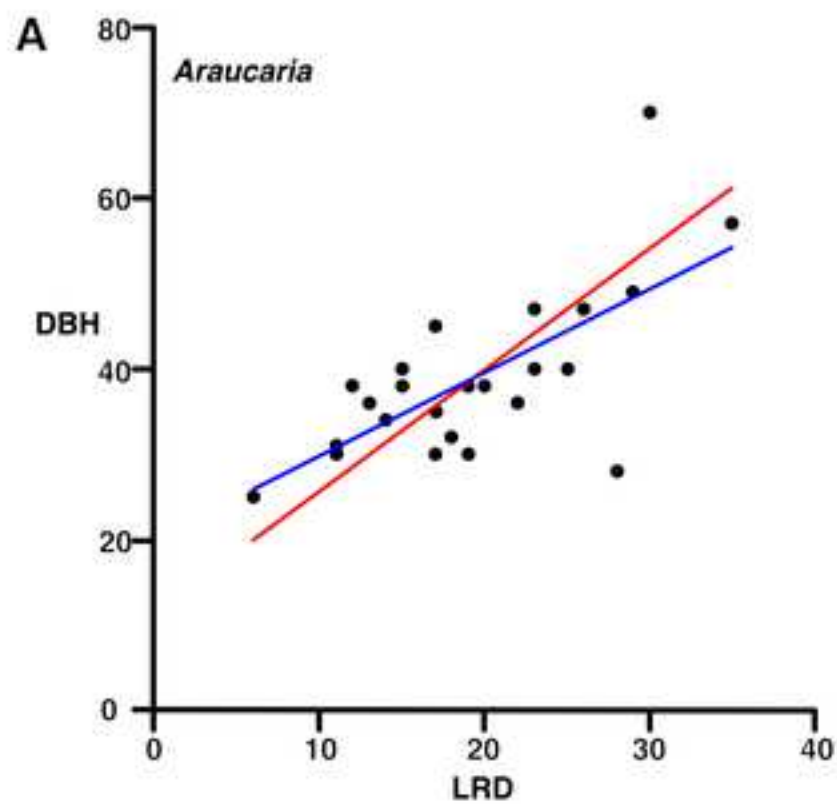




Figure S1. Aerial photographs of the Cairo site

The site now shows new gravel cover and surface weathering. Some root systems were partially re-excavated for views with a drone in order to indicate relative sizes of the individuals identified [in Figure 1C](#). Vehicle is 5.7 m length for scale.

(A) Overhead view with individuals a-f identified, arrows.

(B), Oblique view looking north, individuals b-e identified, arrows.

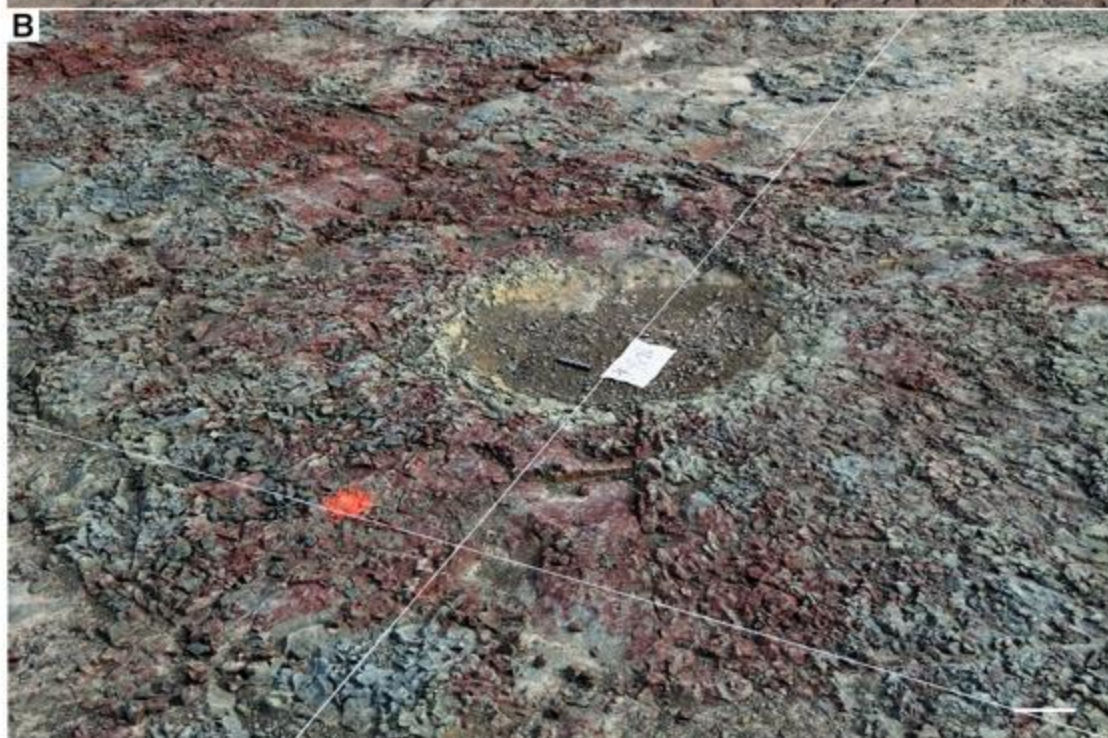


Figure S2. *Eospermatopteris* root systems

(A) Individual within the overwash siltstone ([Figure 1C](#), arrow a within region IV), and also in [Figures 3A-B](#). The image also shows core holes 11 and 12 along with red iron oxide stain derived from drilling the paleosol below. A radiating pattern of roots is apparent on the surface as well as the boundary with subvertical slickened sides marking the boundary of root bound sediment. Scale bar, 10 cm.

(B) Right hand individual in the group labeled b within region I in [Figure 1C](#) at the time of mapping. Center of system with 5 cm scale is partly filled with exogenous sediment and has a yellowish limonite stain. The surrounding raised root mass is shows mottling and abundant root halos. Scale bar, 10 cm.

(C) Same individual as (A), showing boundary of root mass with subvertical slickensides. Scale bar, 1 cm.



Figure S3. *Archaeopteris* root system, individual e in [Figure 1C](#)

(A) Aerial view of showing root system center, arrow, in region II, with limonite staining of region III to the right, as described in the text. Scale bar, 1 m.

(B) Root system approximately midway between center and tip, showing more-or-less equal dichotomy of a structural root. Scale bar, 3 cm.

(C) Root system near (B), showing complex branching and overlaps of structural roots. Scale bar, 5 cm.



Figure S4. *Archaeopteris* root system, individual e in [Figure 1C](#), showing finer scale roots.

(A) Structural root at mid level showing attachment of smaller root, arrow, similar in size to those bearing lateral small roots interpreted as part of a feeder root system. Scale bar, 2 cm.

(B) Small root bearing very fine root, arrow. Scale bar, 1 cm.

(C) Root similar in size to (B) with attachment of lateral root, arrow. Scale in photo, 5 cm.

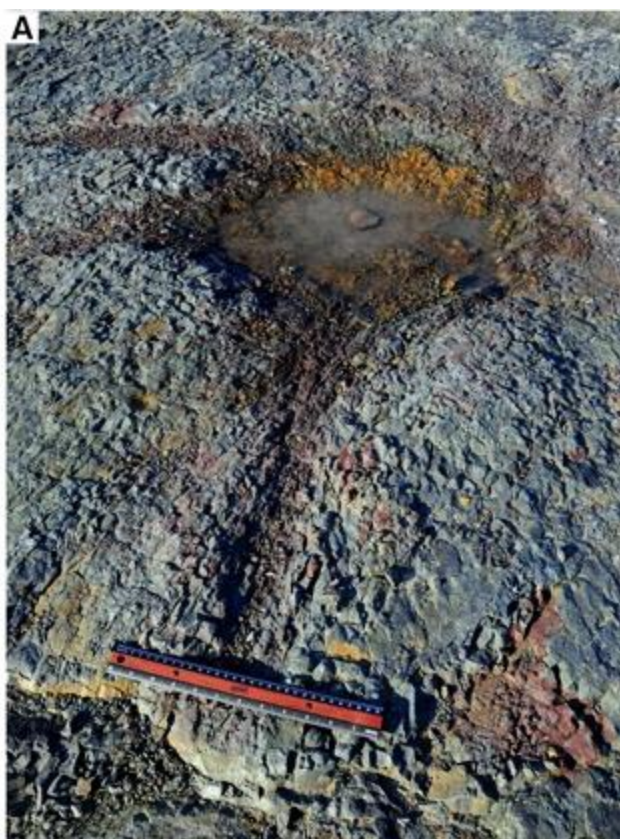


Figure S5. Lycopsid? root system, individual c in [Figure 1C](#)

(A) Oblique view of root system center showing a radiating system of primary roots, and slickenside boundary immediately in front of the ruler (1 ft = 30.5 cm) for scale.

(B) Rootlets with longitudinal striations on root mass immediately adjacent and attached to the primary root in the foreground in (A). Scale bar, 1 cm.

(C) Tip of secondary root, as described in the text, with attached rootlets. This region is the same as in [Figure 6F](#), but imaged instead wet with oblique daylight. Scale bar, 5 mm.

(D) Higher magnification of rootlet near that in (B). Scale bar, 5 mm.

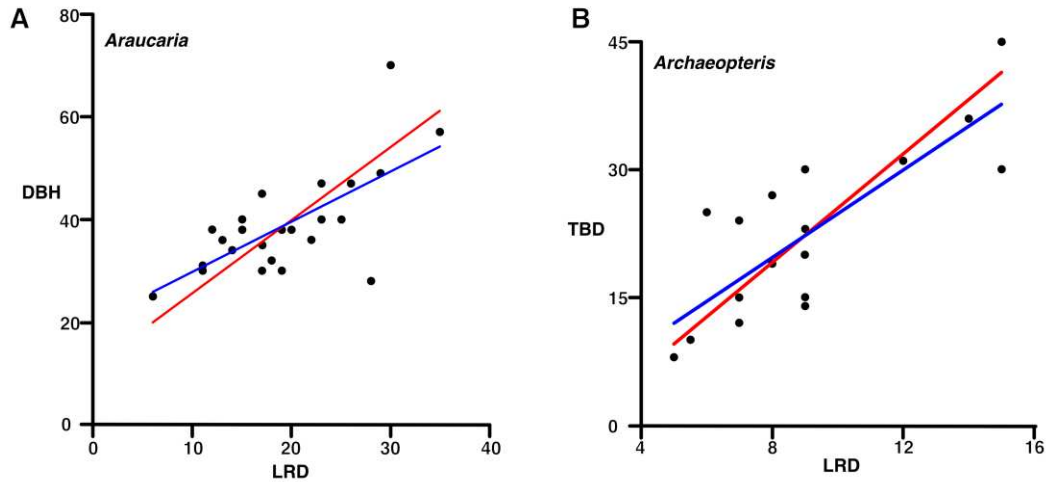


Figure S6. Regressions utilized in estimating size of *Archaeopteris* trees at Cairo Quarry.

(A) Using *Araucaria* as proxy for trunk taper. Diameter of the largest measured lateral root for each tree observed on the soil surface (LRD) versus diameter at breast height (DBH) converted from measured circumference. Regression predictions are represented by red line ($DBH = (1.4206)LRD + 11.392$) for RMA regression, and blue line ($DBH = (0.9772)LRD + 19.984$) for linear regression (LM).

(B) *Archaeopteris* field observations; diameter of the largest measured lateral root for each root system (LRD) versus diameter of the trunk base for each root system (TBD). Regression predictions are represented by red line ($TBD = (3.1859)LRD - 6.4176$) for RMA regression, and blue line ($TBD = (2.5682)LRD - 0.8756$) for linear regression (LM).

Loc	TBD	LRD	RMA DBH	LM DBH	RMA H	LM H	TBD H
X14	45	15	32.70	34.64	26.02	26.93	31.51
Q9	40	14	31.28	33.66	25.33	26.47	29.36
M16	31	12	28.44	31.71	23.93	25.54	25.20
V17	30	15	32.70	34.64	26.02	26.93	24.70
P11	30	9	24.18	28.78	21.70	24.10	24.70
O18	27	8	22.76	27.80	20.93	23.60	23.19
I19	25	6	19.92	25.85	19.32	22.59	22.14
T1	30	7	21.34	26.82	20.14	23.10	24.70
E24	23	9	24.18	28.78	21.70	24.10	21.06
R6	20	9	24.18	28.78	21.70	24.10	19.37
M19	19	8	22.76	27.80	20.93	23.60	18.78
G25	15	9	24.18	28.78	21.70	24.10	16.30
W10	16	7	21.34	26.82	20.14	23.10	16.94
K1	15	7	21.34	26.82	20.14	23.10	16.30
N17	14	9	24.18	28.78	21.70	24.10	15.64
E28	14	7	21.34	26.82	20.14	23.10	15.64
F30	12	5.5	19.21	25.36	18.90	22.33	14.26
Z17	8	5	18.50	24.87	18.48	22.08	11.18

Table S1. Regression estimate of *Archaeopteris* tree heights

Key to columns:

- Loc** Grid location of individual on map (Figure 1C).
TBD Trunk base diameter measured in the field (cm).
LRD Maximum diameter of roots attached to the tree base (cm).
DBH Diameter of trunk at breast height estimated from
RMA or, **LM** Regressions of *Araucaria* (cm).
H Height of tree derived from DBH as estimated from
RMA or, **LM** Regressions of *Araucaria* (m).
H Height of tree estimated directly from **TBD** (m).